

SURGERY IN COLORED TENSOR MODELS

CARLOS I. PÉREZ-SÁNCHEZ

ABSTRACT. Rooted in group field theory and matrix models, random tensor models are a recent background-invariant approach to quantum gravity in arbitrary dimensions. Colored tensor models (CTM) generate random triangulated orientable (pseudo)-manifolds. We analyze, in low dimensions, which known spaces are triangulated by specific CTM interactions. As a tool, we develop a graph-encoded surgery that is compatible with the quantum-field-theory-structure and use it to prove that a single model, the complex φ^4 -interaction in rank-2, generates all orientable 2-cobordisms, thus, in particular, also all orientable, closed surfaces. We show that certain quartic rank-3 CTM, the φ_3^4 -theory, has as boundary sector all closed, possibly disconnected, orientable surfaces. Hence all closed orientable surfaces are cobordant via the φ_3^4 -theory.

CONTENTS

1. Introduction	1
2. Tensors models and their graph theory	3
2.1. Homology of colored graphs	7
2.2. Jackets and degree-computations	8
2.3. The boundary graph	11
2.4. The realization of colored graphs	12
2.5. Ribbon and 3-colored graphs	13
3. Graph Surgery	15
3.1. Colored graph surgery	15
3.2. Matrix-models as tensor-models	17
4. The boundary sector of the φ_3^4 -theory	21
4.1. Completeness of the boundary sector	21
5. Conclusions	27
Acknowledgement	28
Appendix A. Computing homology of colored graphs	29
Appendix B. The cell complex of a ribbon graph	30
References	34

1. INTRODUCTION

Colored tensor models (CTM) have recently flourished as a random-geometry framework that has proven the ability to model quantum gravity in arbitrary dimensions [1, 20, 36, 35], partially following the line of thought of 2-dimensional quantum gravity modeled by random matrices [15]. CTMs are quantum field theories for tensorial objects with forbidden symmetries, which has been called *color*. The bridge is, essentially,

$$Quantum \rightarrow Random \quad \text{and} \quad Gravity \rightarrow Graph\text{-encoded geometry}.$$

The Euclidean path integral formulation of CTM defines a measure that facilitates the first correspondence. The second ‘map’ is a simplicial version of the known General

Relativity correspondence for $D \geq 2$, whose simplicial analogue is the Regge action in terms of the deficit angles [7], here expressed in a graph-theoretical context. The Feynman graphs of colored tensor models have enough structure to encode a sensible space and both correspondences harmonically coexist. This entitles this framework to generate ‘weighted triangulations of (pseudo)manifolds’¹.

In a historical vein, the term *color*, introduced by di Francesco [14], appeared first, as many conceptions in tensor models do, in the context in the theory of matrix models. In that setting colors stand for the different sizes of rectangular matrix fields. The idea that ‘coloring’ forbids certain index-contractions was successfully carried on by Gurău [20], who introduced several ‘colored’ tensor fields, extending di Francesco’s idea to the context of Group Field Theories [17, 30] in order to exclude graphs that could not reasonably encode spaces. The additional tensor fields can be integrated out, thus obtaining an effective action for a single field (see e.g. [14, Sec. 5]), which, however, retains the colored structure. Nowadays (*random*) *tensor models* stands for a rather boarder cluster of alike theories [40, 11, 10] with physically promising features, empowered by the large- N expansion in *Gurău’s degree* [23, 21], and excelling in renormalization techniques [5, 18, 31, 6, 10].

Parallel to the fairly vivid study of the QFT-techniques of tensor models, a ‘geometry-quota’ should also be achieved. Thus, the study of the geometry and topology of the graph theory of tensor models should be also addressed.

At the core of the link between graph theory and geometry that concerns us, lies *Pezzana’s theorem* [34] on manifold crystallization. It allows piecewise linear manifolds to be represented by graphs with more of information, the so-called *colored graphs*. These colored graphs are precisely the Feynman graphs of colored tensor models. Thus, after Gurău’s work [20, 22], Pezzana’s theorem yields a surjection

$$\{\text{All rank-}D \text{ tensor model actions } S_{\text{int}}\} \longrightarrow \{\text{PL-}D\text{-manifolds}\}.$$

What Pezzana’s theorem does not specify is the tensor-model action that generates the graphs that represent certain class of manifolds. In physics one commonly scrutinizes a single model. Therefore it is interesting to pose the following question:

$$\textit{Given a class of manifolds, which CTM-action generates it?} \quad (\star)$$

The action should be polynomial by physical reasons. Thus, given a subcategory \mathcal{C} of manifolds (up to equivalence \sim), one wishes to find a tensor-model action S_{int} and to prove the surjectivity of the composition

$$\{\text{Feynman diagrams of } S_{\text{int}}\} \hookrightarrow \{(D+1)\text{-colored graphs}\} \xrightarrow{\Delta} \mathcal{C}/\sim,$$

where Δ is a ‘manifold reconstruction’-scheme (see Sec. 2.4 and [16]). Techniques like the bubble-homology of graphs [20] assist in distinguishing spaces (see Sec. 2.1) and shall be used here.

We fix now the setting to answer (\star) in low dimensions, that is, we choose the right family member of tensor models². Since we want to prove a surjectivity, the result is stronger if we keep the classes of graphs emerging in that framework at its minimum,

¹ Pseudomanifolds are simplicial complexes that are non branching, pure and strongly connected. Since we aim at the construction of actual PL-manifolds, we do not deepen in that concept. Moreover we work here in dimensions 2 and 3 and piecewise linear manifolds is all we need, by Moise’s theorem [27]. Thus, henceforth we only write ‘manifold’.

² The generation of graphs and their characteristics are dependent on the type, structure and field chosen of tensor model chosen, i.e. whether it is colored, or hybrid, as multi-orientable tensor models [41]; and the vector spaces where the tensors are defined can also over \mathbb{R} or \mathbb{C} .

which means a large-symmetry in the action. The right choice is the complex CTM, as exposed in Section 2.

Having chosen the setting, we choose now the potential S_{int} . We work with rank-2 and rank-3 tensor models and in both instances we take a quartic potentials (which due to their distinct structures of look quite different).

Our strategy is mainly surgery: In certain categories of manifolds, by using surgery of graphs one is able to generate new spaces and readily compute some topological invariants of them from the properties of their parts. It is therefore desirable to have this in the context of graphs. The existent concept in the context of the graph theoretical representation of piecewise linear manifolds by Pezzana, Gagliardi, Ferri *et al.* [16]—to our knowledge the only available concept—unfortunately does not respect the QFT-structure of tensor models, as we show here (Sec. 3, Rem. 3.4). We develop a QFT-compatible and CTM-compatible surgery aiming at answering (\star) for dimension 2, but we went further also to dimension 3. What we concretely obtained is:

- A well-defined 3-colored graph surgery (Definition 3.1), which is faithful to its topological realization (Lemma 3.2).
- The generation of all closed, connected orientable surfaces from (vacuum graphs of) the rank-2 *quartic* potential (Lemma 3.6). This stronger than the \mathbb{R} -matrix model case, as, say, the following graph



of the real quartic matrix model is forbidden in any complex rank-2 theory.

- The generation of all orientable 2-cobordisms by the same quartic potential (Theorem 3.10), more generally, if one allows surfaces with boundary.

Working in one dimension higher, we lift the surgery of 3-colored graphs to an operation on open 4-colored graphs and use this operation to prove that:

- Boundary graphs of *a certain* quartic rank-3 model, the so-called φ_3^4 -theory, generate all closed, connected orientable surfaces. That is, those surfaces are null-bordant in the sense of the φ_3^4 -theory (Proposition 4.1).
- More generally, any two compact, orientable closed, *possible disconnected* surfaces are 3-cobordant in by (a space reconstructed from) certain φ_3^4 -Feynman graph (Theorem 4.6).

This article has the following structure. We motivate first, in Section 2, the study of colored graphs by introducing from scratch, albeit quite straightforwardly, colored tensor models. A rather lengthy introduction on the graph theoretical machinery shall be provided there. The reader which is familiar with CTM can skip that section. Examples there (which we do not skimp on) shall become useful later on, though. Sections 3 and 4 are the core, where we prove our claims above. The reader that does not feel familiar with graph-homology and/or ribbon graphs might find useful Appendices A and B, respectively.

2. TENSORS MODELS AND THEIR GRAPH THEORY

Colored tensor models are quantum field theories for tensorial objects specified by an integer D and by so-called *interaction vertices*. The integer $D \geq 2$ is the rank of tensors fields $\varphi : \mathcal{H}_1 \otimes \mathcal{H}_2 \otimes \cdots \otimes \mathcal{H}_D \rightarrow \mathbb{C}$ on products of Hilbert spaces $\mathcal{H}_1, \dots, \mathcal{H}_D$ and the

interaction vertices $\{\text{Tr}_{\mathcal{B}_\alpha}(\varphi, \bar{\varphi})\}_\alpha$ are determined by invariance under products of unitary groups $\mathcal{U}(\mathcal{H}_1) \times \mathcal{U}(\mathcal{H}_2) \times \cdots \times \mathcal{U}(\mathcal{H}_D)$, as we now explain. Renormalization should care for a second selection-process. While the following discussion and definitions can be carried out without any effort to arbitrary rank, for sake of concreteness we restrict ourselves to rank-3, thus considering tensors $\varphi, \bar{\varphi} : \mathcal{H}_1 \otimes \mathcal{H}_2 \otimes \mathcal{H}_3 \rightarrow \mathbb{C}$. We also assume for simplicity, that \mathcal{H}_c are large but finite dimensional.

For any integer $c = 1, 2, 3$, which one calls *color*, take a basis $\{\vartheta_c^a : a \in I_c\}$ of the dual of \mathcal{H}_c . Here each $I_c \subset \mathbb{Z}$ serves as an index set, which will be often obviated. We let $\varphi =: \sum_{a_1, a_2, a_3} \varphi_{a_1 a_2 a_3} \vartheta_1^{a_1} \otimes \vartheta_2^{a_2} \otimes \vartheta_3^{a_3}$. Each color- c index a_c transforms independently under a change of basis of \mathcal{H}_c . The coordinates transform therefore under unitary elements $W^{(c)} \in \mathcal{U}(\mathcal{H}_c)$ like

$$\begin{aligned}\varphi'_{a_1 a_2 a_3} &= \sum_{b_1, b_2, b_3} W_{a_1 b_1}^{(1)} W_{a_2 b_2}^{(2)} W_{a_3 b_3}^{(3)} \varphi_{b_1 b_2 b_3}, \\ \bar{\varphi}'_{a_1 a_2 a_3} &= \sum_{b_1, b_2, b_3} \overline{W}_{a_1 b_1}^{(1)} \overline{W}_{a_2 b_2}^{(2)} \overline{W}_{a_3 b_3}^{(3)} \bar{\varphi}_{b_1 b_2 b_3}.\end{aligned}$$

We take as classical action only invariants under the group $\mathcal{U}(\mathcal{H}_1) \times \mathcal{U}(\mathcal{H}_2) \times \mathcal{U}(\mathcal{H}_3)$, so $S[\varphi, \bar{\varphi}] = \sum_\alpha \text{Tr}_{\mathcal{B}_\alpha}(\varphi, \bar{\varphi})$. The only quadratic invariant,

$$S_0 = \text{Tr}_2(\varphi, \bar{\varphi}) := \sum_{a_1, a_2, a_3} \bar{\varphi}_{a_1 a_2 a_3} \varphi_{a_1 a_2 a_3}, \quad (2.1)$$

is understood as the kinetic term³. Higher order terms like

$$\text{Tr}_{\mathcal{V}_2}(\varphi, \bar{\varphi}) = \lambda \sum_{\mathbf{a}, \mathbf{b}, \mathbf{p}, \mathbf{q}} \bar{\varphi}_{q_1 q_2 q_3} \bar{\varphi}_{p_1 p_2 p_3} (\delta_{a_1 p_1} \delta_{b_1 q_1} \delta_{a_2 q_2} \delta_{b_2 p_2} \delta_{a_3 p_3} \delta_{b_3 q_3}) \varphi_{a_1 a_2 a_3} \varphi_{b_1 b_2 b_3} \quad (2.2)$$

are the interaction vertices. By Schur's Lemma the tensors in the trace can be contracted only with δ 's (or multiples thereof, which can be absorbed in the *coupling constant* λ). The explicit expression of each one of these $\text{Tr}_{\mathcal{B}_\alpha}$ has certain number (say k) of fields $\bar{\varphi}_{\mathbf{p}^1}, \dots, \bar{\varphi}_{\mathbf{p}^k}$, which are fully contracted with same number of fields $\varphi_{\mathbf{a}^1}, \dots, \varphi_{\mathbf{a}^k}$, where $\mathbf{p}^i = (p_1^i, p_2^i, p_3^i)$, $\mathbf{a}^i = (a_1^i, a_2^i, a_3^i) \in I_1 \times I_2 \times I_3$ for each $i = 1, \dots, k$.

Here it is handy, in order to avoid writing these long expressions, to represent these vertices using either *stranded* graphs or their *colored, bipartite* version. The former is obtained as follows: each invariant trace must contain $\varphi_{a_1 a_2 a_3}$ and the complex conjugate field $\bar{\varphi}_{p_1 p_2 p_3}$. We represent these graphically by associating them a bunch of $D = 3$ white nodes with outgoing strands and a bunch of $D = 3$ dark nodes with incoming strands respectively:

$$\varphi_{a_1 a_2 a_3} \mapsto \begin{array}{c} \text{green} \\ \text{red} \\ \text{blue} \end{array} \text{ and } \quad \bar{\varphi}_{p_1 p_2 p_3} \mapsto \begin{array}{c} \text{blue} \\ \text{red} \\ \text{green} \end{array} \text{ (reversed order)}$$

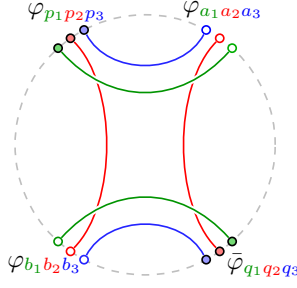
We associate to each δ single lines, in such a way that $\delta_{a_1 p_1} = \xrightarrow{\text{green}}$ connects the color-1 (green) strands of $\bar{\varphi}_{p_1 p_2 p_3}$ and $\varphi_{a_1 a_2 a_3}$; $\delta_{a_2 p_2} = \xrightarrow{\text{red}}$ connects the color-2 (red) strands and

³ In future work it will also consider a slightly modified trace with a symmetry-breaking term E , though:

$$S[\varphi, \bar{\varphi}] = \text{Tr}_2(\bar{\varphi}, E\varphi) + \sum_\alpha \text{Tr}_{\mathcal{B}_\alpha}(\varphi, \bar{\varphi}),$$

with $E : \mathcal{H}_1 \otimes \mathcal{H}_2 \otimes \mathcal{H}_3 \rightarrow \mathcal{H}_1 \otimes \mathcal{H}_2 \otimes \mathcal{H}_3$ 'self-adjoint', $\text{Tr}_2(\bar{\varphi}, E\varphi) = \text{Tr}_2(E\bar{\varphi}, \varphi)$. The first term is distinguished, and being quadratic in φ , it represents the kinetic part of the action, where E could be interpreted as the Laplacian. This allows to state Group Field Theories, via Fourier-transform, as colored tensor models.

$\delta_{a_3 p_3} = \xrightarrow{3}$ those of color 3 (blue). Therefore the trace in eq. (2.2) is



It turns out that these graphs are still somehow quite elaborate and we will opt for even more simplified graphs that contain the same information. To the interactions one associates finite regularly edge-3-colored vertex-bipartite graphs. This picture is obtained from the stranded representation of graphs by collapsing the nodes $\circ \bullet \circ$ of $\varphi_{a_1 a_2 a_3}$ to a single white vertex \circ , and those of $\bar{\varphi}_{p_1 p_2 p_3}$, i.e. $\bullet \circ \bullet$, to a black vertex \bullet . Accordingly, the three strands of $\varphi_{a_1 a_2 a_3}$ join at \circ , and those of $\bar{\varphi}_{p_1 p_2 p_3}$ at \bullet , like

$$\varphi_{a_1 a_2 a_3} \mapsto \begin{array}{c} a_3 \\ \curvearrowright \\ \circ \\ \curvearrowleft \\ a_2 \end{array}, \quad \bar{\varphi}_{p_1 p_2 p_3} \mapsto \begin{array}{c} p_2 \\ \curvearrowleft \\ \bullet \\ \curvearrowright \\ p_3 \end{array}. \quad (2.3)$$

To the δ 's one associates numbered, or in the parlance *colored*, strands. Then the i -colored strand \xrightarrow{i} for $\delta_{a_i p_i}$ joins a_i and p_i in the vertices (2.3), so that, for instance

$$\text{Tr}_{\mathcal{V}_2}(\varphi, \bar{\varphi}) = \begin{array}{c} \circ \bullet \circ \\ \curvearrowright \quad \curvearrowleft \\ \circ \bullet \circ \end{array} = \begin{array}{c} 3 \\ \circ \quad \circ \\ \curvearrowright \quad \curvearrowleft \\ 1 \quad 1 \\ \curvearrowleft \quad \curvearrowright \\ \bullet \quad \bullet \\ 2 \quad 2 \\ \curvearrowleft \quad \curvearrowright \\ 3 \end{array} \quad (2.4)$$

This completes the comments on notation of interaction vertices; now we address the notation of the Feynman graphs of these theories. The partition function reads⁴

$$Z[J, \bar{J}] = \frac{\int \mathcal{D}\varphi \mathcal{D}\bar{\varphi} e^{\text{Tr}(\bar{J}\varphi) + \text{Tr}(\bar{\varphi}J) - S[\varphi, \bar{\varphi}]}{\int \mathcal{D}\varphi \mathcal{D}\bar{\varphi} e^{-S[\varphi, \bar{\varphi}]}} , \quad \mathcal{D}\varphi \mathcal{D}\bar{\varphi} := \prod_{\mathbf{a} \in I_1 \times I_2 \times I_3} \frac{d\varphi_{\mathbf{a}} d\bar{\varphi}_{\mathbf{a}}}{2\pi i}. \quad (2.5)$$

The quantity $d\mu(\varphi, \bar{\varphi}) = \mathcal{D}\varphi \mathcal{D}\bar{\varphi} \exp(-S_0[\varphi, \bar{\varphi}])$ defines a Gaussian measure. Parenthetically, $d\mu$ and its perturbations, as other quantities can be formally studied in probability (see [24], where a tensor version of the Dyson-Wigner law is obtained) but that is beyond the our aim in this paper.

The perturbative expansion yields the Wick's contraction of products of powers of the form $[\text{Tr}_{\mathcal{B}_{\alpha_i}}(\varphi, \bar{\varphi})]^{n_i}$ of the interaction vertices, i.e. all different fully Wick-contracted terms obtained of the integrals of

$$[\text{Tr}_{\mathcal{B}_{\alpha_1}}(\varphi, \bar{\varphi})]^{n_1} [\text{Tr}_{\mathcal{B}_{\alpha_2}}(\varphi, \bar{\varphi})]^{n_2} \cdots [\text{Tr}_{\mathcal{B}_{\alpha_p}}(\varphi, \bar{\varphi})]^{n_p}, \quad (n_i \in \mathbb{Z}_{>0}).$$

The corresponding Feynman diagrams are $(3+1)$ -colored graphs (Sec. 2.1). It is illustrative to see how one arrives to that result departing from the stranded representation.

⁴ Actually the partition function has a factor N^{D-1} in front of the action $S[\varphi, \bar{\varphi}]$ in a more realistic scenario, and the measure should be rescaled accordingly. Here we work with the graph structure of the theory and thus the factor can be restored anytime. See Remark 2.9 below.

Remark 2.1. The representations above have a slightly deceiving terminology. The graph \mathcal{G} in the left of (2.9) is called *uncolored graph* [39, Sec. 1.3]; the graph in the right is denoted by $\mathcal{G}_{\text{color}}$ or \mathcal{G}_c and is the colored version of \mathcal{G} . These terminology is also well explained in [5, Def. 1 and Fig. 5]. Sometimes, avoiding the stranded representation, \mathcal{G} is represented as \mathcal{G}_c with lines that are fainted if they are c -colored ($c \neq 0$), but we refrain from doing so. In the initial version of colored tensors a collection of D random tensors, rather than a single one as here, was considered. Then $D - 1$ of them were integrated out, and what one remains with is an ‘uncolored’ [8] tensor model with another (effective) action, which however, had still the colors encoded in their indices. The difference is that the geometric realization for $\mathcal{G}_{\text{color}}$ includes a *face* for each loop in 2 arbitrary colors—either $0c$ or cd , for $c, d = 1, \dots, D$ ($c \neq d$). For the uncolored version, one considers the loops of colors $0c$; the equivalence of notations, as in (2.9), explains why. We shall no longer use the stranded representation and prefer the ‘colored one’, for which, however, we drop the label in $\mathcal{G}_{\text{color}}$ and use instead \mathcal{G} directly.

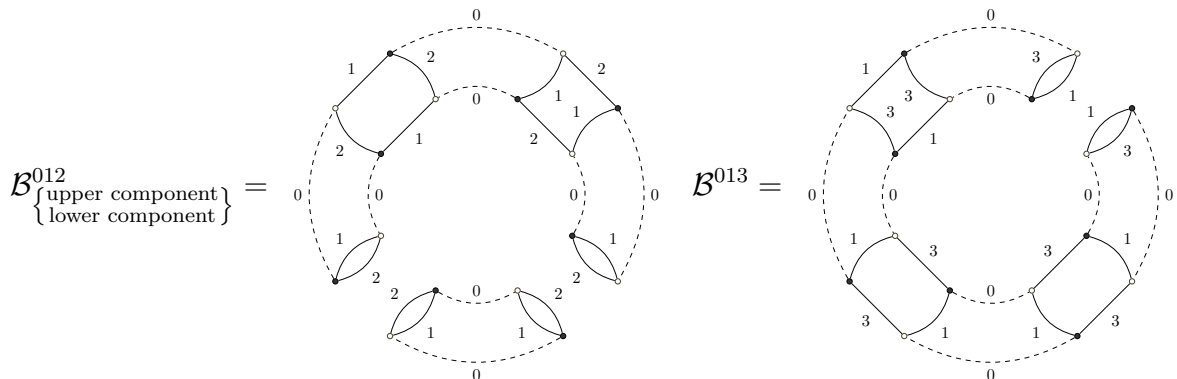
2.1. Homology of colored graphs. The theory of homology that assigns topological meaning to the Feynman graphs of colored tensor models has been defined by Gurău [20] and is referred to as bubble-homology. That name is due to:

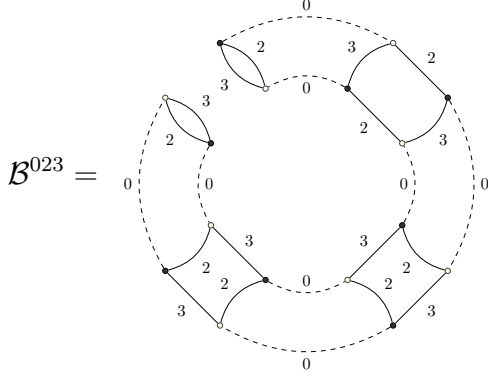
Definition 2.2. By a D -colored graph, \mathcal{G} , one understands here a graph $\mathcal{G} = (\mathcal{G}^{(0)}, \mathcal{G}^{(1)})$ with the following properties:

- i) *Bipartiteness:* The *vertex set* is finite $\mathcal{G}^{(0)}$ and bipartite: $\mathcal{G}^{(0)} = \mathcal{G}_w^{(0)} \cup \mathcal{G}_b^{(0)}$, where $\mathcal{G}_w^{(0)}$ are the *white*, and $\mathcal{G}_b^{(0)}$ the *black* vertices. Further, any $e \in \mathcal{G}^{(1)}$ is attached to precisely one black vertex w and one white vertex, b , which we write $s(e) = b, t(e) = w$ or just $e = \overline{bw}$.
- ii) *Regular coloring:* The *edge set* is partitioned as $\mathcal{G}^{(1)} = \cup_{c=1}^D \mathcal{G}_c^{(1)}$. The elements of $\mathcal{G}_c^{(1)}$ are said to have color c ; this coloration is *regular*, i.e. there are D edges incident to any vertex having different colors.

We denote by $\text{Grph}_{\text{col},D}$ the set of connected D -colored graphs and by $\text{IIGrph}_{\text{col},D}$ the set of disconnected D -colored graphs. Graphs in $\text{Grph}_{\text{col},D}$ are also sometimes called *closed*. A p -*bubble* \mathcal{B} of $\mathcal{G} \in \text{Grph}_{\text{col},D}$ is a connected subgraph of \mathcal{G} in p colors ($1 \leq p \leq D$), that is a subgraph \mathcal{B} of \mathcal{G} in $\text{Grph}_{\text{col},p}$ (the p colors being a subset of $\{1, \dots, D\}$).

Example 2.3. Let \mathcal{G} be the Feynman graph (2.9). Then $\mathcal{G} \in \text{Grph}_{\text{col},3+1}$, \mathcal{G} having colors $\{0, 1, 2, 3\}$. The number of 0-bubbles (indexed by $\mathcal{G}^{(0)}$) is 16; it also has 32 1-bubbles, 8 of each color $c = 0, \dots, 3$ (indexed by $\mathcal{G}^{(1)}$); there are 24 2-bubbles sitting in \mathcal{G} : 3 bubbles of colors $\{01\}$ and $\{02\}$ each; 2 bubbles of colors $\{03\}$, 6 bubbles with colors $\{12\}$ and 5 with colors $\{13\}$ and $\{23\}$ each. The eight 3-bubbles are drawn here:





$$\begin{aligned} \mathcal{B}_1^{123} &= \mathcal{V}_1, & \mathcal{B}_2^{123} &= \mathcal{V}_2, \\ \mathcal{B}_3^{123} &= \mathcal{V}_3, & \mathcal{B}_4^{123} &= \mathcal{V}_3. \end{aligned}$$

One defines the *chain complex* of the graph \mathcal{G} as the collection of groups $C_p(\mathcal{G}; \mathbb{Z}) = \text{span}_{\mathbb{Z}}\{\mathcal{B} \mid \mathcal{B} \text{ is a } p\text{-bubble}\}$, for $p = 0, \dots, D$. Hence, in the case of the example above $C_0(\mathcal{G}) = \mathbb{Z}^{16}$, $C_1(\mathcal{G}) = \mathbb{Z}^{32}$, $C_2(\mathcal{G}) = \mathbb{Z}^{24}$, $C_3(\mathcal{G}) = \mathbb{Z}^8$. The boundary maps are given as follows. Let $I = (i_1, \dots, i_p)$ be a fully ordered subset of $\{0, 1, \dots, D\}$ and let $\kappa(I)$ be the number of bubbles with edge-color set I . Each of those bubbles is fully determined⁵ by additionally specifying a connected component, e.g. through its vertex-set, which we denote by $\mathcal{V}_r(I) \subset \mathcal{G}^{(0)}$. Here the integer $r = 1, \dots, \kappa(I)$ indexes all possible vertex-sets with colors I . Any bubble in $C_p(\mathcal{G}, \partial_p)$ has then the form $\mathcal{B}_{\mathcal{V}_r(I)}^I$. The *boundary map* is

$$\partial_p(\mathcal{B}_{\mathcal{V}_r(I)}^{(i_1, \dots, i_p)}) = \sum_{q=1}^p (-1)^{q+1} \sum_{\mathcal{W} \subset \mathcal{V}_r(I^p)} \mathcal{B}_{\mathcal{W}}^{i_1 \dots \widehat{i_q} \dots i_p} \quad \text{where } (p \geq 2).$$

The inner sum is performed over all the vertex-subsets \mathcal{W} of $\mathcal{V}_r(I^p)$ with colors $i_1 \dots \widehat{i_q} \dots i_p$. For arbitrary p we write then:

$$\partial_p(\mathcal{B}_{\mathcal{V}}^{I^p}) = \begin{cases} 0 & \text{if } p = 0, \\ v - \bar{v} & \text{if } p = 1, \text{ and } \bar{v} = t(\mathcal{B}_{\mathcal{V}}^{I^p}), v = s(\mathcal{B}_{\mathcal{V}}^{I^p}) \\ \sum_{q=1}^p (-1)^{q+1} \sum_{\mathcal{W}_{\widehat{i_q}}} \mathcal{B}_{\mathcal{W}_{\widehat{i_q}}}^{i_1 \dots \widehat{i_q} \dots i_p} & \text{if } p \geq 2 \end{cases} \quad (2.10)$$

and the restriction to $\mathcal{W}_{\widehat{i_q}} \subset \mathcal{V}_r(I^p)$ on the sum is implicit. Thus, one orients the edges e from the white (sources $s(e)$) into the black vertices (targets $t(e)$). We are now able to define:

Definition 2.4. The *Euler characteristic* $\chi(\mathcal{G})$ of a colored graph \mathcal{G} is $\sum_q (-1)^q \text{rk} H_q(\mathcal{G})$.

Examples of the homology of graphs and the respective Euler characteristic follow. We also refer to Appendices A and B, for more detailed computations.

2.2. Jackets and degree-computations.

Definition 2.5. (Jackets and degree.) Let \mathcal{G} be a $(D+1)$ -colored bipartite graph. Each cycle $\tau = (\ell_0 \dots \ell_D) \in \mathfrak{S}_{D+1}$, defines a graph \mathcal{J}_τ called *jacket* as follows: \mathcal{J}_τ has the same sets of vertices and edges as \mathcal{G} ,

$$\mathcal{J}_\tau^{(0)} := \mathcal{G}^{(0)}, \quad \mathcal{J}_\tau^{(1)} := \mathcal{G}^{(1)},$$

but its faces are those faces of \mathcal{G} (i.e. two-bubbles) that have colors $(\ell_{i+1} \ell_0)$ or $(\ell_i \ell_{i+1})$ with $i = 0, \dots, D$:

$$\mathcal{J}_\tau^{(2)} = \{f \in \mathcal{G}^{(2)} \mid f \text{ has colors } (\tau^q(0), \tau^{q+1}(0)), q \in \mathbb{Z}\}.$$

⁵Actually (consistently) overdetermined, since a single vertex is enough to determine a connected component.

Here τ^q stands for $\tau \circ \dots \circ \tau$ applied (q times) to the color 0. By definition, $\mathcal{J}_\tau^{(k)} = \emptyset$ for $k > 2$, so that jackets are ribbon graphs. Since τ and τ^{-1} lead to the same face-sets, $\mathcal{J}_\tau^{(2)} = \mathcal{J}_{\tau^{-1}}^{(2)}$, those cycles are considered equivalent. Hence \mathcal{G} has $D!/2$ jackets. By computing their bubble-homology one finds, for certain non-negative integer $g_{\mathcal{J}}$,

$$H_q(\mathcal{J}) = \begin{cases} \mathbb{Z} & \text{if } q = 0, 2, \\ \mathbb{Z}^{2g_{\mathcal{J}}} & \text{if } q = 1, \\ 0 & \text{if } q > 2. \end{cases}$$

i.e. the Euler characteristic of the geometric realization of \mathcal{J} is $2 - 2g_{\mathcal{J}}$.

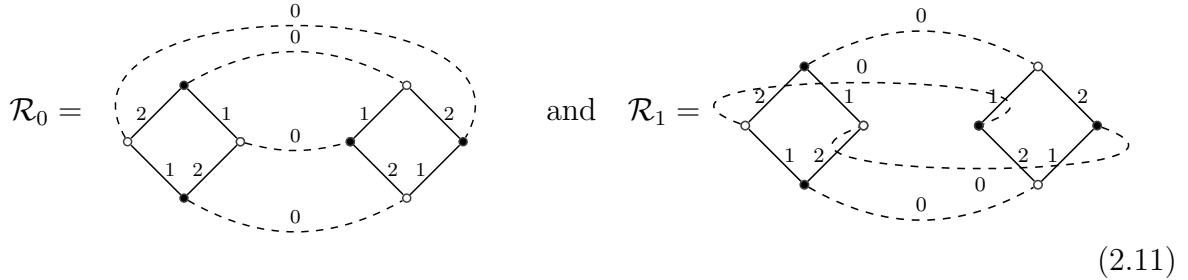
Definition 2.6. The *Gurău's degree* of a closed graph $\mathcal{G} \in \text{Grph}_{\text{col}, D+1}$ ($D \geq 2$) is defined as the sum of all the genera of the jackets of \mathcal{G} :

$$\omega(\mathcal{G}) = \sum_{\mathcal{J} \subset \mathcal{G}} g_{\mathcal{J}}.$$

A graph \mathcal{G} with $\omega(\mathcal{G}) = 0$ is called *melon*.

To fully understand the concept of jacket the next brief examples might help.

Example 2.7. The case $D = 2$. There, $(2 + 1)$ -colored graphs have a single jacket, the ribbon graph itself. The degree $\omega(\mathcal{R})$ is therefore precisely the genus $g(\mathcal{R})$. This will allow to treat matrix models as a rank-2 tensor model, as specified below 3.2. Consider the next graphs



arising in the $\mathcal{O}(\lambda^2)$ -terms from of the evaluation of the quartic rank-2 CTM,

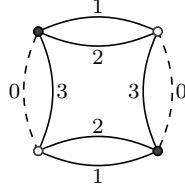
$$\int \mathcal{D}[\varphi, \bar{\varphi}] \exp(-\text{Tr}(\bar{\varphi}\varphi) - \lambda \text{Tr}((\bar{\varphi}\varphi)^2)),$$

where the 0-colored lines are Wick's contractions. The homology of \mathcal{R}_0 can be computed, but one can directly use its (dual) cell complex $\Delta(\mathcal{R}_0)$ directly: the vertices and edges of the graph are the 0-cells and 1-cells of $\Delta(\mathcal{R}_0)$, respectively; to any bicolored path, one glues a 2-cell. Then $\Delta(\mathcal{R}_0)$ turns out to be a sphere. The graph \mathcal{R}_1 requires a slightly more detailed computation (see A.1 in appendix A). From its homology $H_0(\mathcal{R}_1) = \mathbb{Z}$, $H_1(\mathcal{R}_1) = \mathbb{Z}^2$, $H_2(\mathcal{R}_1) = \mathbb{Z}$, one infers that \mathcal{R}_1 is a (dual triangulation of a) torus.

Example 2.8. (When is a graph non-melonic?) There are at least four non-equivalent criteria to test non-melonicity:

- (i) Find a non-melonic subbubble $\mathcal{B}_{(\kappa_0)}^{\hat{D}}$ and use $\omega(\mathcal{G}) \geq D \sum_{\kappa} \omega(\mathcal{B}_{(\kappa)}^{\hat{D}})$ (see [24, Lemma 1] or [8, Prop. 2]), where κ indexes all 3-bubbles with colors \hat{D} .
- (ii) Since melonic graphs can be shown to be necessary dual to spheres [23, Lemma 4], one can compute the homology $H_{\star}^{\text{bubble}}(\mathcal{G})$ and show that it is not isomorphic to the (say cell-) homology $H_{\star}^{\text{cell}}(\mathbb{S}^3)$ of a sphere.
- (iii) Compute the genera of the jackets of \mathcal{G} .
- (iv) Face-counting (cf. [8, Prop. 1] and [32]).

Contrary to matrix models, tensor models turn out to encode more than topology. That can be noted in the following example. Let \mathcal{G} be the following necklace-graph⁶ in four colors:



For this graph, (i) above does not help. Since all four bubbles $\mathcal{B}^0, \dots, \mathcal{B}^3$ are the same as the vertices \mathcal{V}_i . Thus those bubbles are melonic, and the lower bound given by (i) is trivially satisfied — by definition, $\omega(\mathcal{G})$ is already a non-negative integer. The other three last methods are listed in decreasing order of difficulty (but not by implication). To begin with (ii) the chain complex is

$$0 \xrightarrow{\partial_4=0} C_3(\mathcal{G}) \simeq \mathbb{Z}^4 \xrightarrow{\partial_3} C_2(\mathcal{G}) \simeq \mathbb{Z}^8 \xrightarrow{\partial_2} C_1(\mathcal{G}) \simeq \mathbb{Z}^8 \xrightarrow{\partial_1} C_0(\mathcal{G}) \simeq \mathbb{Z}^4 \xrightarrow{\partial_0=0} 0.$$

Taking homology yields (see A.2 appendix A)

$$H_3(\mathcal{G}) = \mathbb{Z}, \quad H_2(\mathcal{G}) = 0, \quad H_1(\mathcal{G}) = 0, \quad H_0(\mathcal{G}) = \mathbb{Z}.$$

That method still does not help to know whether the graph is melonic, since \mathcal{G} has the same homology as \mathbb{S}^3 . Proceeding with (iii), one has for the jackets $\mathcal{J}_\tau, \mathcal{J}_\pi, \mathcal{J}_\sigma$ corresponding to $\tau = (0123), \pi = (0213), \sigma = (0132) \in \mathfrak{S}_4$, the following groups:

$$\begin{aligned} H_2(\mathcal{J}_\tau) &= \mathbb{Z}, & H_1(\mathcal{J}_\tau) &= 0, & H_0(\mathcal{J}_\tau) &= \mathbb{Z}, \\ H_2(\mathcal{J}_\pi) &= \mathbb{Z}, & H_1(\mathcal{J}_\pi) &= \mathbb{Z}^2, & H_0(\mathcal{J}_\pi) &= \mathbb{Z}, \\ H_2(\mathcal{J}_\sigma) &= \mathbb{Z}, & H_1(\mathcal{J}_\sigma) &= 0, & H_0(\mathcal{J}_\sigma) &= \mathbb{Z}. \end{aligned}$$

Therefore $\omega(\mathcal{G}) = 1$. Of course this is consistent with the face-counting formula [7, eq. 2.9] for rank- D theories:

$$F_{\mathcal{G}} := \#(\mathcal{G}^{(2)}) = \binom{D-1}{2} \cdot \frac{\#(\mathcal{G}^{(0)})}{2} + (D-1) - \frac{2\omega(\mathcal{G})}{(D-2)!},$$

which in this case ($D = 4 = \#(\mathcal{G}^{(0)}), F_{\mathcal{G}} = 8$) also yields $\omega(\mathcal{G}) = 1$. By Proposition 4.3 of [25] (namely, four-colored graphs possessing a spherical jacket J , i.e. $g_J = 0$, are themselves spherical) one has a counterexample for the reciprocal of ‘being a melon implies being dual to a sphere’. In [37] it has been found that the jackets represent embedded matrix theories in the tensor theories. Moreover the jackets are interpreted as the surface along which a Heegaard splitting takes place. Here we found an example of this explicit splitting for the three-sphere. The genus-0 jackets \mathcal{J}_τ and \mathcal{J}_σ correspond to the genus-0 Heegaard splitting of $\mathbb{S}^3 \subset \mathbb{C}^2$, that is, the coordinates (z_1, z_2) of \mathbb{S}^3 with $\Im(z_2) = 0$, i.e. \mathbb{S}^2 inside \mathbb{S}^3 . The jacket \mathcal{J}_π is the genus-1 Heegaard splitting of \mathbb{S}^3 , the Clifford torus \mathbb{T}^2 , given by the locus $|z_1| = \sqrt{2}/2 = |z_2|$.

Remark 2.9. (On the importance of melons). So far we have considered the action functional as frozen, not flowing with the energy scale, N . This large integer is defined as follows. One usually sets the Hilbert spaces \mathcal{H}_c all to the fundamental representation of $U(N)$. One keeps in mind the color as an artifact that forbids elements in one factor

⁶The name ‘necklace’ has been borrowed from [9].

of $U(N) \times U(N) \times U(N)$ to jump to another one. The action (without sources) is then scaled as

$$Z_0 = \int \mathcal{D}\varphi \mathcal{D}\bar{\varphi} e^{-N^{D-1} S[\varphi, \bar{\varphi}]} . \quad (2.12)$$

Melons are the dominating graphs, for the amplitude of a graph \mathcal{G} is weighted [22] by Gruău's degree as

$$\mathcal{A}(\mathcal{G}) \sim N^{D - \frac{2\omega(\mathcal{G})}{(D-1)!}} . \quad (2.13)$$

This is the tensor version of the well-known genus-weighted amplitudes of ribbon graphs \mathcal{R} in matrix models, $\mathcal{A}(\mathcal{R}) \sim N^{2-2g(\mathcal{R})}$. Having ribbon graphs a single jacket, the latter formula is a particular case of Formula (2.13), with $D = 2$.

2.3. The boundary graph.

Definition 2.10. A graph \mathcal{G} is an *open* $(D+1)$ -colored graph (with colors $c = 0, 1, \dots, D$) if its vertex-set is bipartite in the following two senses:

- (i) As before, $\mathcal{G}^{(0)} = \mathcal{G}_w^{(0)} \cup \mathcal{G}_b^{(0)}$, where $\mathcal{G}_w^{(0)}$ are the *white*, and $\mathcal{G}_b^{(0)}$ the *black* vertices,
- (ii) any vertex is either *inner* or *outer*, $\mathcal{G}^{(0)} = \mathcal{G}_{\text{inn}}^{(0)} \cup \mathcal{G}_{\text{out}}^{(0)}$; moreover, the set $\mathcal{G}_{\text{inn}}^{(0)}$ of inner vertices is regular with valence $D + 1$ and outer vertices have valence 1.

Additionally, the edge set $\mathcal{G}^{(1)}$ is $(D + 1)$ -colored—that is $\mathcal{G}^{(1)} = \cup_{c=0}^D \mathcal{G}_c^{(1)}$, where $\mathcal{G}_c^{(1)}$ is the set of color- c edges—and satisfies the following:

- (iii) for each color c and each inner vertex $v \in \mathcal{G}_{\text{inn}}^{(0)}$, there is exactly one color- c edge, $e \in \mathcal{G}_c^{(1)}$, attached to v ,
- (iv) each external vertex is connected to the graph only by a color-0 edge.

Both the leaves of open graphs and the edges that are attached to them shall be referred to as *external legs*. We also let

$$\text{Grph}_{\text{col}, D+1}^{(\mathcal{N})} := \{ \mathcal{G} \text{ open } (D+1)\text{-colored} \mid \#(\mathcal{G}_{\text{out}}^{(0)}) = \mathcal{N} \} . \quad (2.14)$$

In the models we treat here, being the graphs bipartite, \mathcal{N} is even. We allow $\mathcal{N} = 0$, setting $\text{Grph}_{\text{col}, D+1}^{(0)} := \text{Grph}_{\text{col}, D+1}$. To complete the notation, given an open graph \mathcal{G} one can extract a (generally non-regular) colored graph $\text{inn}(\mathcal{G})$ defined by

$$\text{inn}(\mathcal{G})^{(0)} = \mathcal{G}_{\text{inn}}^{(0)} \quad \text{inn}(\mathcal{G})^{(1)} = \mathcal{G}^{(1)} \setminus \{ \text{external legs of } \mathcal{G} \} . \quad (2.15)$$

The graph $\text{inn}(\mathcal{G})$ is called *amputated* graph.

Therefore alternative notations might include omission of the outer vertices ('half lines') or their replacement by sources. There, to each non-contracted black (resp. white) vertex, a source J (resp. \bar{J}) is attached). For instance the following graph, at the right of which we represent its amputation, is open:

$$\mathcal{G} = \begin{array}{c} J_a \quad \bar{J}_a \\ \vdots \quad \vdots \\ \text{---}0 \quad 0\text{---} \\ \text{---}1 \quad 2 \\ \text{---}0 \quad 0\text{---} \\ \text{---}1 \quad 2 \end{array} \quad \text{inn}(\mathcal{G}) = \begin{array}{c} \text{---}1 \quad 2 \\ \text{---}0 \quad 0\text{---} \\ \text{---}1 \quad 2 \end{array} \quad (2.16)$$

In the QFT-context, open graphs are not-fully Wick-contracted interaction vertices.

Definition 2.11. A *colored tensor model* $V(\varphi, \bar{\varphi})_D$ is determined by an integer $D \geq 2$, called *dimension*, which is given by the rank of the tensors, and by an *action*

$$V(\varphi, \bar{\varphi})_D = \sum_{\mathcal{B} \in \Upsilon} \lambda_{\mathcal{B}} \text{Tr}_{\mathcal{B}}(\varphi, \bar{\varphi}) ,$$

where $\Upsilon \subset \text{Grph}_{\text{col},D}$ is a finite subset and $\lambda_B \in \mathbb{R}$. The set of *connected Feynman diagrams* of the model $V(\varphi, \bar{\varphi})_D$ is denoted by $\mathfrak{Feyn}_D(V)$ or $\mathfrak{Feyn}_D(V(\varphi, \bar{\varphi}))$. It satisfies

$$\mathfrak{Feyn}_D(V) = \{ \mathcal{G} \in \cup_{k=0}^{\infty} \text{Grph}_{\text{col},D+1}^{(2k)} \mid \text{inn}(\mathcal{G})^{\hat{0}} \in \Upsilon \}.$$

The graphs in $\text{Grph}_{\text{col},D+1}^{(0)} \cap \mathfrak{Feyn}_D(V) = \text{Grph}_{\text{col},D+1} \cap \mathfrak{Feyn}_D(V)$ are called *vacuum graphs* of the model V . We write $\mathfrak{Feyn}_D^{\mathbb{R}}(V)$ if the tensor field is real.

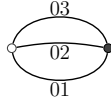
The boundary shall be defined in such a way that its geometric realization matches the boundary of the geometric realization of the graph. Thus, the boundary of a graph is defined to be empty on a vacuum (i.e. closed) graphs and on open graphs as follows.

Definition 2.12. Let \mathcal{G} be an open Feynman diagram of a rank- D colored tensor field theory. The *boundary graph* $\partial\mathcal{G}$ of \mathcal{G} has by definition the following vertex and edges sets:

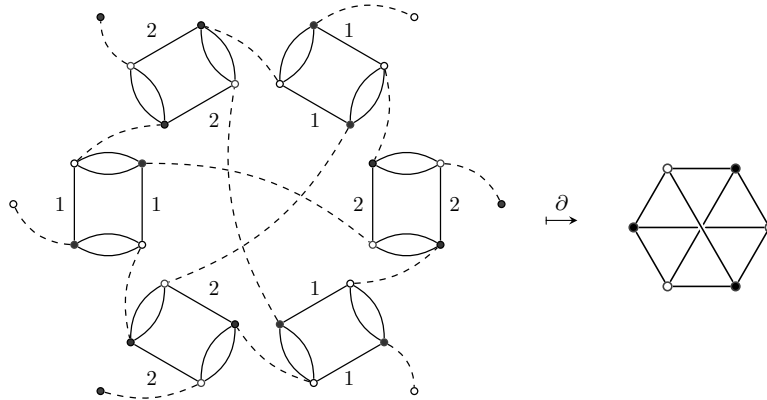
$$(\partial\mathcal{G})^{(0)} = \mathcal{G}_{\text{out}}, \quad (\partial\mathcal{G})^{(1)} = \cup_{c=1}^D (\partial\mathcal{G})_c^{(1)}, \quad \text{with } (\partial\mathcal{G})_c^{(1)} = \{(0c)\text{-colored paths in } \mathcal{G}\}.$$

Another conventions define $(\partial\mathcal{G})^{(0)}$ as the set of external lines. Since an external line goes to an outer vertex, both definitions are equivalent. The definition also says that the outer vertices are the leaves of the graph.

Example 2.13. The graph \mathcal{G} in eq. (2.16) has two outer vertices, and by the previous construction, $\partial\mathcal{G}$ will have two vertices. For each $c = 1, 2, 3$, an edge of color c connects those, since there is a $(0c)$ -bicolored path between the two outer vertices \mathcal{G} . Then $\partial\mathcal{G}$ is



which does not differ (but apparently in labelling) from the graph of the propagator. A slightly more interesting example is



The boundary graph might be also disconnected, as we will easily see (in Lemma 4.4, constructively).

2.4. The realization of colored graphs. One can construct a colored triangulation $\Delta(\mathcal{G})$ of compact piecewise-linear manifolds departing from $D + 1$ -colored graphs \mathcal{G} . The simplicial (pseudo)complex $\Delta(\mathcal{G})$ is assembled as follows [16]:

- for each $v \in \mathcal{G}^{(0)}$, $\Delta(\mathcal{G})$ has a D -simplex σ_v
- one labels the vertices σ_v by the colors $\{0, 1, \dots, D\}$

- for each color c and each edge $e_c \in \mathcal{G}_c^{(1)}$ one identifies the faces $\sigma_{s(e_c)}$ and $\sigma_{t(e_c)}$ that do not contain the color c (i.e. the $(D-1)$ -simplices that lie opposite to the vertex labelled by c)

Because colored graphs allow multiple edges, D -simplices might intersect at more than one face (whence the prefix *pseudo*). With some abuse on notation, we write $\Delta(\mathcal{G})$ also for $M = |\Delta(\mathcal{G})|$, the manifold that $\Delta(\mathcal{G})$ triangulates. We say that \mathcal{G} *represents* M .

Remark 2.14. In the 2-dimensional case the cell complex associated to ribbon graphs and 3-colored graphs exposed in Appendix B is the Poincaré dual of this Δ -construct. Since we basically analyze the Euler characteristic of graphs, this has no effect.

Colored graph theory also incarnates the coning $X \mapsto CX$ of a topological space [22]. If \mathcal{B} is a D -colored graph, then one defines $C\mathcal{B}$ as the open $(D+1)$ -colored graph with $(C\mathcal{B})_{\text{inn}}^{(0)} = \mathcal{B}^{(0)} \times \{0\}$ and $(C\mathcal{B})_{\text{out}}^{(0)} = \mathcal{B}^{(0)} \times \{1\}$ (a second copy of the vertices). Moreover, if $v \in \mathcal{B}^{(0)}$ is white (resp. black) then $(v, 0)$ is white (resp. black) as well, but $(v, 1)$ is black (resp. white). The edges are defined by

$$(C\mathcal{B})^{(1)} = \mathcal{B}^{(1)} \cup \{\text{single color-0 edge between } (v, 0) \text{ and } (v, 1) \mid v \in \mathcal{B}^{(0)}\}$$

The cone is defined so that $\Delta(C\mathcal{B}) = C\Delta(\mathcal{B})$. The relation $\partial(C\mathcal{B}) = \mathcal{B}$ holds also for each graph.

2.5. Ribbon and 3-colored graphs. Ribbon graphs are also known as *fat graphs*. We choose a definition and notation inspired by [29, 28], but we will really need only a subset of those graphs, which arises either as Feynman diagrams in matrix models or as boundary-graphs of Feynman graphs of rank-3 tensor field theories. In all generality, though:

Definition 2.15. [28] A *ribbon graph* is a finite graph without isolated vertices nor leaves, together with a cyclic ordering of the set of half-edges at each vertex.

The definition includes, implicitly, the following set of data and conditions:

- two finite sets: the *vertex-set* $\mathcal{R}^{(0)}$, and the *half-edges set* $\mathcal{R}^{(1/2)}$
- a map $p : \mathcal{R}^{(1/2)} \rightarrow \mathcal{R}^{(0)}$. The picture of ' $p(h) = v$ ' is that the half-edge h emanates from v .
- $n_v := |p^{-1}(v)|$ is called the *valence* of a vertex v and the condition $n_v > 1$ is imposed. Thus \mathcal{R} has neither isolated vertices ($n_v \neq 0$), nor leaves ($n_v \neq 1$).
- a cyclic orientation of $\mathcal{R}^{(1/2)}$.
- an involution j on the set of half-edges; here $j(h) = h'$ means that $\{h, h'\}$ is a full edge—if so then, of course, $j(h') = j^2(h) = h$. Moreover, it is imposed that j has no fixed point.

The usual graph notion in terms of vertices and (full) edges, $\mathcal{R} = (\mathcal{R}^{(0)}, \mathcal{R}^{(1)})$, is then recovered by defining $\mathcal{R}^{(1)}$, the *edge-set*, as the set of cycles of j [29]. Without loss of generality we write

$$\mathcal{R}^{(1/2)} = \{(v, \alpha) : v \in \mathcal{R}^{(0)}, \alpha = 1, \dots, n_v\} \quad \text{and} \quad p = \text{pr}_1.$$

Since each edge e is determined by two half-edges $h, h' \in \mathcal{R}^{(1/2)}$ that are joined (i.e. $j(h) = h'$), e can be rewritten as $e = [h, h'] = [h', h]$. If $e = [(v, \alpha), (w, \beta)]$, think of e as

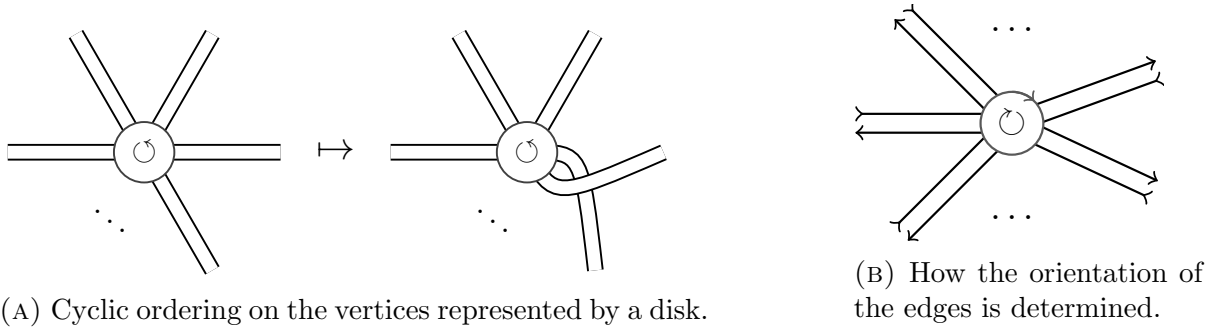


FIGURE 1.

being attached to the vertex v at the α -th place, and to the vertex w in the β -th place.

Before formally constructing the cell-complex for a ribbon graph, we motivate in an informal vein their usual notation from the abstract definition. For a vertex $v \in \mathcal{R}^{(0)}$ of valence n_v , the cyclic ordering sees the following operation:

$$\begin{array}{ccc}
 \begin{array}{c} \diagup \\ 2 \\ \diagdown \\ 3 \\ \vdots \\ 4 \\ \vdots \\ n_v \end{array} & \xrightarrow{\quad} & \begin{array}{c} \diagup \\ 2 \\ \diagdown \\ 3 \\ \vdots \\ 4 \\ \vdots \\ n_v \\ 1 \end{array}
 \end{array} \tag{2.17}$$

In order to keep track of the order, the incidence relations are usually graphically represented as follows: edges are *ribbons*, that is rectangles (topological disks D^2); vertices are *disks*. The map j represents the attachment of one side of a half-edge to a disk, as in Fig. 1 (A), thus keeping track of the operation (2.17). The cyclic ordering of the vertex determines an orientation on half-edges–rectangles as shown in Fig. 1 (B) and the ribbons should be drawn taking into account the orientation on both ends. Moreover, the ribbons do not intersect and the way they are attached to the disks must respect the orientation. If we represent the graph on the plane, mismatch of orientations is represented by lines \asymp , which do cross. Nevertheless, crucially, the graph can be drawn without intersections on other surfaces. The lowest-genus closed, orientable surface on a ribbon graph \mathcal{R} can be planarly drawn on is its geometric realization, $\Sigma(\mathcal{R})$ (see App. B).

Definition 2.16. We write $\chi(\mathcal{R})$ for the *Euler characteristic* of the geometric realization of \mathcal{R} , that is $\chi(\mathcal{R}) = \chi(\Sigma(\mathcal{R}))$. In turn, this also defines the *genus* $g(\mathcal{R})$ of \mathcal{R} .

Example 2.17. We illustrate the concepts in the last paragraph for the following simple ribbon graphs:

$$\mathcal{R} = \text{two disks with two parallel ribbons between them}, \quad \mathcal{Q} = \text{two disks with two parallel ribbons between them}, \quad \mathcal{P} = \text{two overlapping disks}.$$

Their ribbon representation is the following (thought of as filled vertices and ribbons):

$$\mathcal{R} = \text{two disks with two parallel ribbons between them, oriented}, \quad \mathcal{Q} = \text{two disks with two parallel ribbons between them, oriented}, \quad \mathcal{P} = \text{two overlapping disks, oriented}.$$

Thus, the fat graph \mathcal{R} has only one boundary component, so $\chi(\Sigma(\mathcal{R})) = 0$. Thus \mathcal{R} can only be planarly drawn on a torus. Also \mathcal{P} has genus 1, as it has only one boundary component, one vertex and two edges (ribbons). The graph \mathcal{Q} has genus 0. The notation we will choose from now on is the omission of the disks, usual in the physics literature, as well as disregarding crossings \asymp . With that notation, \mathcal{P} is shown in graph 1.1. This does not affect the previously defined quantities, because they are homotopy invariant.

Lemma 2.18. *Regularly edge-3-colored, vertex-bipartite graphs are ribbon graphs.*

Proof. Let $\mathcal{G} = (\mathcal{G}^{(0)}, \mathcal{G}^{(1)})$ be a 3-colored graph. We exhibit \mathcal{G} 's ribbon graph structure. The set of vertices of the ribbon graph is the same, $\mathcal{G}^{(0)}$. Define the set of half-edges $\mathcal{G}^{(1/2)} := \mathcal{G}^{(0)} \times \mathbb{Z}_3$, where $\mathbb{Z}_3 = \{1, 2, 3\}$. The map $p : \mathcal{G}^{(1/2)} \rightarrow \mathcal{G}^{(0)}$ is the projection $p = \text{pr}_1$, which satisfies $n_v > 1$ for each vertex $v \in \mathcal{G}^{(0)}$, since $p^{-1}(v) = \mathbb{Z}_3$. We let the cyclic order for white [resp. black] vertices be (123) [resp. (321)]. Finally, the involution j on $\mathcal{G}^{(1/2)}$ is defined as follows: given $h = (v, c) \in \mathcal{G}^{(1/2)}$, let $e \in \mathcal{G}^{(1)}$ be the edge of color c at v (because of regularity and coloring, e is uniquely determined) and w the other vertex e is attached to. Then let $j(h) := (w, c)$. The map j is an involution, since any two vertices can be connected only by one edge. \square

The converse of the previous lemma does not hold. For instance, consider the graph \mathcal{P} in Example 2.17 (or in 1.1). That ribbon graph is not bipartite, since it is a graph of a real φ^4 -matrix model. Regular colored bipartite graphs in more colors can be also given the structure of a ribbon graph, however the cell-attachment does not stop at dimension 2. This explains why having exactly 3 colors is important.

3. GRAPH SURGERY

We develop elementary colored-graph-encoded surgery. The aim of this concept is twofold. The physical motivation is to see that we can expand the free energy $\log(Z[J, \bar{J}])$ of the model in sources indexed by ribbon graphs, having as goal the Ward Identity of the φ_3^4 -theory [33]. We will see here that this expansion is optimal after the identification of those ribbon boundary-graphs with closed, possibly disconnected Riemannian surfaces. The second aim, also for future work, is a macroscopic realization of the theory. This surgery shall become useful as for computing the space the final gluing of a large number of known ‘chunks of space’ represents.

An obstacle to perform this surgery is that one might have not enough simplices; in that case, by removing a simplex (or more), the space might fall apart into a topologically simpler one and information about its topology would be lost. In the same line of thought, there are subtleties concerning disk excision of open graphs (manifolds with boundary). With graphs, by doing what one could naively call ‘removing a disk’ \mathring{D}^n in the wrong place might not create a boundary component \mathbb{S}^{n-1} in the way one expects to do so. This phenomenon is better illustrated by example. Here, in the $\varphi_{D=2}^4$ (matrix)-theory, consider the graph \mathcal{R}_1 of Ex. 2.7. By cutting two color-0 edges one arrives to Figure 2, when one realizes it as a surface. But if one follows any of the two lines of the ‘boundary of the ribbon’ both connect the two boundary components of the surface.

3.1. Colored graph surgery. To prove our statements we need to see how to cut a 2-disk, in this realm, a two-bubble of a graph⁷.

⁷ For instance, take the surface in Figure 2 and put a cap in one of the boundary components (join one ribbon). If one takes two copies of this and tries to glue them along the boundary, and then represent this back as a colored graph, one arrives at definition 3.1

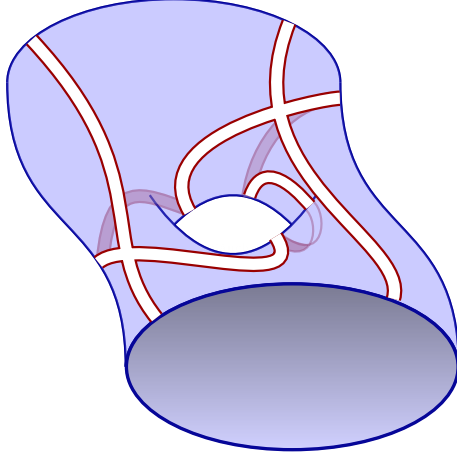


FIGURE 2. If one caps the two boundary components, one obtains \mathcal{R}_1 (Ex. 2.7).

Definition 3.1. Let \mathcal{R} and \mathcal{Q} be (closed) D -colored graphs, $\mathcal{R}, \mathcal{Q} \in \text{Grph}_{\text{col}, D}$. Let c be any color, and e and f be color- c edges in \mathcal{R} and \mathcal{Q} , respectively, i.e. $e \in \mathcal{R}_c^{(1)}$ and $f \in \mathcal{Q}_c^{(1)}$. We define the graph $\mathcal{R}_e \#_f \mathcal{Q}$ as follows:

$$\begin{aligned} (\mathcal{R}_e \#_f \mathcal{Q})^{(0)} &= \mathcal{R}^{(0)} \cup \mathcal{Q}^{(0)}, \\ (\mathcal{R}_e \#_f \mathcal{Q})^{(1)} &= (\mathcal{R}^{(1)} \setminus \{e\}) \cup (\mathcal{Q}^{(1)} \setminus \{f\}) \cup \{e', f'\}, \end{aligned}$$

where e' and f' are c -colored edges defined by $s(e') = s(e)$, $t(e') = t(f)$ and $s(f') = s(f)$, $t(f') = t(e)$ (see Figure 3), which makes $\mathcal{R}_e \#_f \mathcal{Q}$ a connected graph in $\text{Grph}_{\text{col}, D}$. We will often obviate the edges and just write $\mathcal{R} \# \mathcal{Q}$ if this simplification does not lead to confusion.

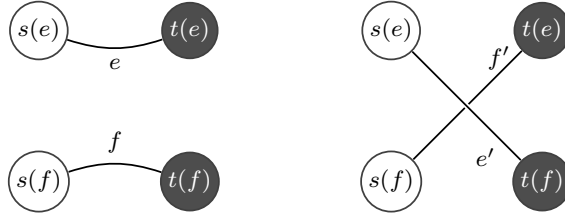


FIGURE 3. On Definition 3.1. Here s and t are source and target. The orientation of the edges is given by setting the ‘white vertices’ as sources.

Lemma 3.2. For any $\mathcal{R}, \mathcal{Q} \in \text{Grph}_{\text{col}, 3}$ and edges e in $\mathcal{R}_c^{(1)}$ and $f \in \mathcal{Q}_c^{(1)}$ of the same color c , the graph $\mathcal{R}_e \#_f \mathcal{Q} \in \text{Grph}_{\text{col}, 3}$ satisfies

$$\chi(\mathcal{R}_e \#_f \mathcal{Q}) = \chi(\mathcal{R}) + \chi(\mathcal{Q}) - 2.$$

Proof. The operation $_e \#_f$ is additive with in vertices and edges. Thus, only the 2-bubbles might change:

$$\chi(\mathcal{R}_e \#_f \mathcal{Q}) = \chi(\mathcal{R}) + \chi(\mathcal{Q}) + (\text{created 2-bubbles} - \text{deleted 2-bubbles}).$$

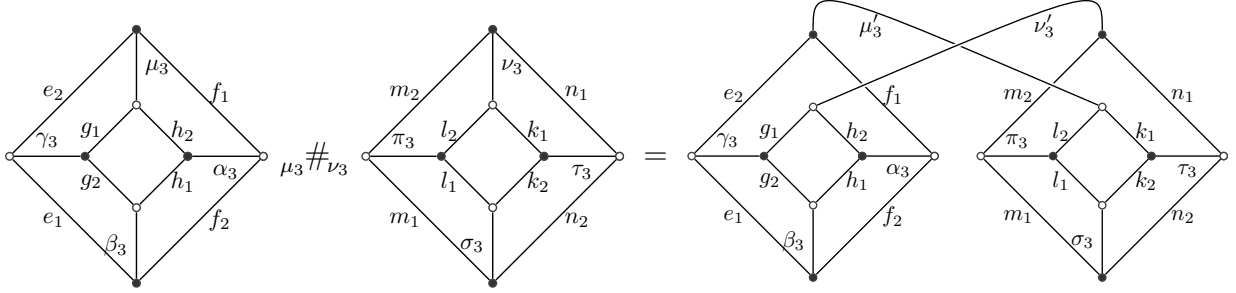
Now, the change in the 2-bubbles can only take place in those containing the edges e or f . Since there are three colors, there are two 2-bubbles of \mathcal{R} , $\mathcal{B}_e^{cd}(\mathcal{R})$, containing e , namely those with colors (cd) , $d \in \{\hat{c}\}$. Similarly, there are two bubbles $\mathcal{B}_f^{cd}(\mathcal{Q})$ containing f . The removal of the edges e and f has as consequence the elimination of the 2-bubbles containing e and f , whence four 2-bubbles are eliminated in the new graph. Now, for

each color $d \neq c$, the new edges e' and f' lie on the same 2-bubble of $\mathcal{R}_e \#_f \mathcal{Q}$. There is exactly one new bubble $\mathcal{B}_{e'f'}^{cd}(\mathcal{R}_e \#_f \mathcal{Q})$ for each d , thus 2 are created in total. Therefore the 2-bubbles decrease in two and the result follows. \square

The previous lemma justifies the notation in previous definition, since for compact, closed n -manifolds M and N one has

$$\chi(M \# N) = \chi(M) + \chi(N) - \chi(\mathbb{S}^n) = \chi(M) + \chi(N) + (-1)^{n+1} - 1.$$

Example 3.3. We perform this first operation on the graphs for a torus and a sphere graphs, namely \mathcal{R}_0 and \mathcal{R}_1 of eq. (2.11), respectively:



Here each subindex of the edges corresponds with its coloring. Moreover, the color 0 has been replaced by 3, since the result holds for graphs in abstract (not only in the QFT context). According to the lemma, $\chi(\mathcal{R}_0 \# \mathcal{R}_1) = \chi(\mathcal{R}_0) + \chi(\mathcal{R}_1) - 2$. The same happens if we contract $\mathcal{R}_0 \# \mathcal{R}_1$ with another copy \mathcal{R}'_0 of \mathcal{R}_0 along the edges σ'_3 and β_3 , respectively. We get then $\Delta((\mathcal{R}_0 \# \mathcal{R}_1) \# \mathcal{R}'_0) \simeq \mathbb{T}^2$. This very graph will be used for the construction in Section 4.

Remark 3.4. If certain $(D + 1)$ -colored graph \mathcal{B} represents a $(D$ -dimensional) manifold M one says that \mathcal{B} is a *crystallization* of M if moreover the number of D -bubbles in \mathcal{B} is exactly $D + 1$; or, rephrasing that condition, if by removing a single arbitrary color $i = 0, \dots, D$, one gets a connected graph $\mathcal{B}^{\hat{i}}$. For example, the necklace graph in Example 2.8 is a crystallization, but the graph (2.9) is not.

The school of graph-theoretical representations of manifolds found a crystallization $\mathcal{B}_M \#_{\text{crys}} \mathcal{B}_N$ of the connected sum $M \# N$ two manifolds, from the crystallizations of \mathcal{B}_M and \mathcal{B}_N of the summands. In the orientable case (i.e. for bipartite graphs), in order to obtain $\mathcal{B}_M \#_{\text{crys}} \mathcal{B}_N$ one deletes two vertices $p \in (\mathcal{B}_M)_w^{(0)}$ and $q \in (\mathcal{B}_N)_b^{(0)}$ and puts together, by color, the half-edges at $s^{-1}(p)$ and $t^{-1}(q)$ created by said vertex-removal.

The issue is that crystallizations are not that abundant in $\mathfrak{Feyn}_D(V)$. But even supposing that certain crystallizations \mathcal{B} and \mathcal{B}' are Feynman diagrams of a model $V(\Phi)$, one cannot guarantee that also $\mathcal{B} \#_{\text{crys}} \mathcal{B}' \in \mathfrak{Feyn}_D(V)$ for the same model, as nothing forces $(\mathcal{B} \#_{\text{crys}} \mathcal{B}')^{\hat{0}}$ to be in the interaction potential V . Proposition 3.5 shows the advantage of using the $\#$ defined above instead.

3.2. Matrix-models as tensor-models. The perturbative expansion of the partition function of the matrix model

$$\int \mathcal{D}[M, \bar{M}] e^{-\text{Tr}(\bar{M}M) - \lambda V(M, \bar{M})}, \quad (3.1)$$

as is well-known, generates ribbon graphs, which are canonically given the structure of a triangulated surface by taking the dual complex of the construction $\Sigma(\mathcal{R})$ in Appendix B. Thus the interaction vertices of

$$S = \text{Tr}(\bar{M}M) + V(M, \bar{M}) = \text{Tr}(\bar{M}M) + \lambda \text{Tr}((\bar{M}M)^p) \quad (3.2)$$

contribute with $(2p)$ -agonal vertices

$$\text{ribbon graph} = \text{dual triangulation to} \text{ ribbon graph} \quad (3.3)$$

ribbon graph in the LHS is due to the construction in Lemma 2.18. We denote by $\mathfrak{Feyn}_2(\varphi^{2p})$ the set of Feynman diagrams of the theory defined by the functional (3.1). Other conventions differ from the one given so far. There, the loop inside the vertex, that is the (12) -colored bubble, is not drawn. For instance, if $p = 2, 3, 4$ one would have the following representation of the vertices:

$$\text{three ribbon graphs} \quad (3.4)$$

that is, the colors $i = 1, 2$ are drawn as simple lines, and the 0-color double. The geometric realization is of course unaltered, since in the only difference is to decide whether one adds a vertex, as in the latter case (cf. (3.4)), or a face, as in the representation (3.3).

A (complex) matrix model here is, in the tensor model context, is a polynomial

$$V(\varphi, \bar{\varphi}) = \sum_{p \in I} \lambda_p \text{Tr}((\varphi \bar{\varphi})^p)$$

for a finite set $I \subset \mathbb{Z}_{>2}$.

Proposition 3.5. *Fix a rank-2 CTM (or a complex matrix model) interaction V . Let \mathcal{R} and \mathcal{Q} be Feynman diagrams of that model. Let $e \in \mathcal{R}_0^{(0)}$ and $f \in \mathcal{Q}_0^{(0)}$. Then $\mathcal{R}_e \#_f \mathcal{Q} \in \mathfrak{Feyn}_2(V)$ as well.*

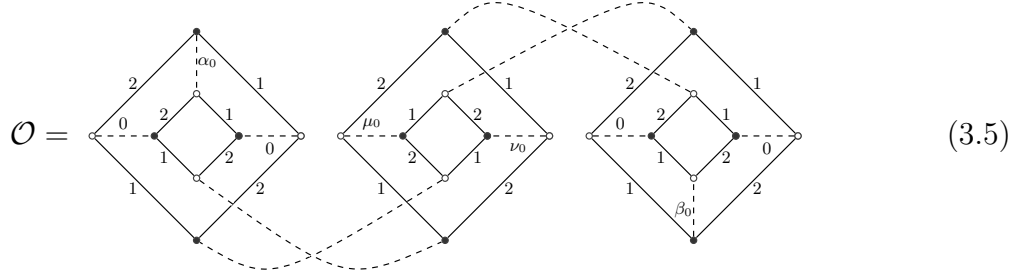
Proof. It is trivial by noticing that 0-colored edges are Wick contractions. \square

Let $\text{Riem}_{c,cl,o}$ be the homeomorphism-classes of connected, closed orientable surfaces. We consider the empty surface also as an element of $\text{Riem}_{c,cl,o}$. Then we claim that the only quartic model $\mathfrak{Feyn}_2^{\mathbb{C}}((\varphi \bar{\varphi})^2)$ has enough graphs to generate all of $\text{Riem}_{c,cl,o}$. A weaker version of the following result corresponding to the real matrix φ^4 -theory might be known. In the complex theory with potential $(\varphi \bar{\varphi})^2$ some graphs of the real theory, $\mathfrak{Feyn}_2^{\mathbb{R}}(\varphi^4)$, are forbidden; nonetheless:

Lemma 3.6. *There is a surjection $\mathfrak{Feyn}_2((\varphi \bar{\varphi})^2) \rightarrow \text{Riem}_{c,cl,o}$.*

Proof. Any vacuum graph \mathcal{G}_0 in $\text{Grph}_{col,2+1}^{(0)} \subset \mathfrak{Feyn}_2((\varphi \bar{\varphi})^2)$ yields the empty surface $\beta(\mathcal{G}_0) \in \text{Riem}_{c,cl,o}$; we exclude this trivial case from now on. Because of the classification of orientable, closed surfaces, $\text{Riem}_{c,cl,o} \simeq \mathbb{Z}_{\geq 0}$, one has to construct a graph for each $g \in \mathbb{Z}_{\geq 0}$. For $g = 0$, the graph \mathcal{R}_0 has been shown to triangulate \mathbb{S}^2 . For $g > 0$ we

proceed differently. Let \mathcal{O} be the following graph:



Then consider g copies $\mathcal{O}^{(1)}, \dots, \mathcal{O}^{(g)}$, of that graph \mathcal{O} with distinguished 0-colored edges μ_0^i and ν_0^i , $i = 1, \dots, g$ as shown above. Then we claim that⁹

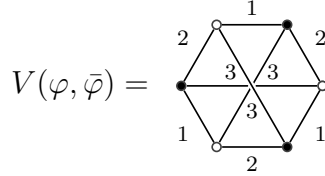
$$\mathcal{Q}_g := \mathcal{O}^{(1)} \#_{\mu_0^1 \nu_0^2} (\mathcal{O}^{(2)} \#_{\mu_0^2 \nu_0^3} (\mathcal{O}^{(3)} \#_{\mu_0^3 \nu_0^4} \dots \#_{\mu_0^{g-2} \nu_0^{g-1}} (\mathcal{O}^{(g-1)} \#_{\mu_0^{g-1} \nu_0^g} \mathcal{O}^{(g)})) \dots) \quad (3.6)$$

has genus g . Indeed, after Lemma 3.2 each sum $\#$ in (3.6) decreases the Euler characteristic in 2. Since each summand \mathcal{O} has $\chi(\mathcal{O}) = 0$ (cf. Example 3.3),

$$\chi(\mathcal{Q}_g) = (g - 1) \cdot \chi(\mathcal{O}) - 2(g - 1) = 2 - 2g. \quad \square$$

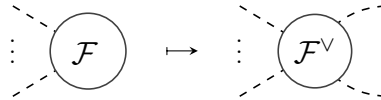
Remark 3.7. By the same token, one can also glue by α_0 and β_0 instead of by μ_0 and ν_0 . The resulting graph $\mathcal{K}_g := \mathcal{O}^{(1)} \#_{\beta_0^1 \alpha_0^2} (\mathcal{O}^{(2)} \#_{\beta_0^2 \alpha_0^3} (\dots \mathcal{O}^{(g-1)} \#_{\beta_0^{g-1} \alpha_0^g} \mathcal{O}^{(g)})) \dots)$ has genus g .

Example 3.8. In view of Lemma 3.6, the rank-3 model with interaction vertex set to \mathcal{Q}_g , for $g \geq 1$ (after properly changing the color 0 into 3), generates no melons at all. A lower-order polynomial interaction with the same characteristic is



This is consequence of the lower-bound for the degree (i), mentioned in example 2.8. Thus in rank-3 theories, an interaction vertex with suitable high degree (e.g. $g = 3$) has degree $\omega(\mathcal{G}) \geq 3$. Thus generation of spheres is not guaranteed (at least not before renormalization, if one does not introduce quadratic counterterms).

Definition 3.9. Let $k \in \mathbb{Z}_{\geq 0}$. For any colored graph \mathcal{F} with $2k$ external legs, $\mathcal{F} \in \text{Grph}_{\text{col}, D+1}^{(2k)}$, pick two vertices $a \in \mathcal{F}_w$ and $p \in \mathcal{F}_b$ joined by a 0-colored edge e_0 . We denote by $\mathcal{F}^\vee(a; p)$ or $\mathcal{F}^\vee(e_0)$ the graph obtained from \mathcal{F} by *opening* the 0-colored edge e_0 . By that we mean that one creates two external legs (or leaves), one at a and one at p , so $\mathcal{F}^\vee(a; p) \in \text{Grph}_{\text{col}, D+1}^{(2k+2)}$. Pictorially,



⁹ One can also do cell-counting: the number of vertices of this graph is $3 \cdot 8 \cdot g$; the number of edges is $3 \cdot 12 \cdot g$ and the number of faces is $|\mathcal{Q}_g^{(12)}| + |\mathcal{Q}_g^{(01)}| + |\mathcal{Q}_g^{(02)}| = 2 + 10 \cdot g$. Indeed, one sees trivially that the (12)-colored bubbles are $3 \cdot 2 \cdot g$. The only non-trivial part is to count the (0i)-bubbles. We see now by induction in the number g of sums $\#$ that the number of (01)-bubbles $|\mathcal{Q}_g^{(01)}|$ is $2g + 1$ and it is also evident that $|\mathcal{Q}_g^{(01)}| = |\mathcal{Q}_g^{(02)}|$.

As usual \overline{ap} and, alternatively, $\overline{\sqcup}p$ stand for Wick contraction (in this context, contraction with a color-0 edge) of the vertices a and p . Thus

$$\mathcal{F}^\vee(\overline{ap}) = \mathcal{F}.$$

and if there is still a 0-colored edge f_0 connecting a black vertex $r \in (\mathcal{F}^\vee(a; p)_{\text{inn}})_b$ with a white one $c \in (\mathcal{F}^\vee(a; p)_{\text{inn}})_w$ one defines

$$\mathcal{F}^\vee(a, c; p, r) := (\mathcal{F}^\vee(a; p))^\vee(c; r) \in \text{Grph}_{\text{col}, D+1}^{(2k+4)}.$$

This graph will be also denoted by $\mathcal{F}^\vee(e_0, f_0)$, when convenient. If moreover $\mathcal{G} \in \text{Grph}_{\text{col}, D+1}^{(2l)}$ and $b = s(f_0) \in \mathcal{G}_w^{(0)}$, $q = t(f_0) \in \mathcal{G}_b^{(0)}$ for certain $f_0 \in \mathcal{G}_0^{(1)}$,

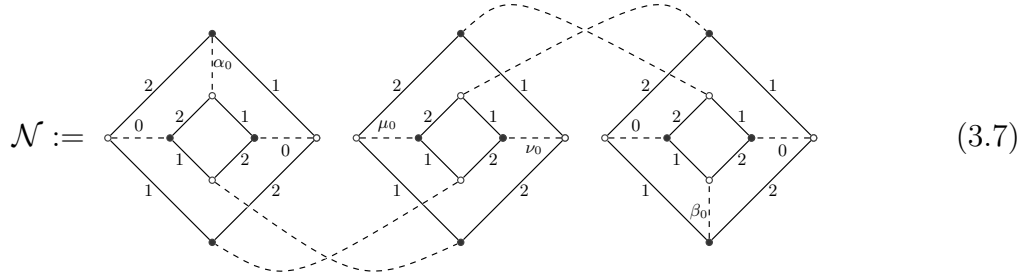
$$\mathcal{F}^\vee(\overline{ap})\overline{\mathcal{G}^\vee(b; q)} \in \text{Grph}_{\text{col}, D+1}^{(2k+2l)}.$$

Notice that this graph is just $\mathcal{F}_{e_0} \#_{f_0} \mathcal{G}$, where $e_0 = \overline{ap}$.

Theorem 3.10. *Let 2-Cob be the set of all orientable 2-cobordisms. There exists a surjection*

$$\xi : \mathfrak{Feyn}_2((\varphi\bar{\varphi})^2) \rightarrow 2\text{-Cob}.$$

Proof. Consider the graph \mathcal{O} in (3.5) and:



Obviously, both graphs are in $\mathfrak{Feyn}_2((\varphi\bar{\varphi})^2)$. Let $M : \sqcup^C \mathbb{S}^1 \rightarrow \sqcup^B \mathbb{S}^1$ be an arbitrary element in 2-Cob. That is, two arbitrary closed 1-manifolds, $\sqcup^B \mathbb{S}^1$ and $\sqcup^C \mathbb{S}^1$ are cobordant via M , a genus- g orientable, compact surface with boundary. We now find a graph $\mathcal{Q}_{g,B,C}$ which (dually) triangulates M .

Remark that the case $B = C = 0$ is the statement in Lemma 3.6. Thus we can suppose $0 < B \leq C$ and set $m := \max\{g, C\} > 0$. Define the following Feynman-graph-valued functions:

$$\mathcal{P} : \{0, 1\} \rightarrow \mathfrak{Feyn}_2((\varphi\bar{\varphi})^2), \quad \mathcal{P}(\epsilon) = \begin{cases} \mathcal{N} & \text{if } \epsilon = 0, \\ \mathcal{O} & \text{if } \epsilon = 1, \end{cases}$$

and

$$\mathcal{S} : \{0, 1\} \times \{0, 1, 2\} \rightarrow \mathfrak{Feyn}_2((\varphi\bar{\varphi})^2), \quad \mathcal{S}(\epsilon, i) = \begin{cases} \mathcal{P}(\epsilon) & \text{if } i = 0, \\ \mathcal{P}(\epsilon)^\vee(\alpha_0) & \text{if } i = 1, \\ \mathcal{P}(\epsilon)^\vee(\alpha_0, \beta_0) & \text{if } i = 2. \end{cases}$$

Notice that the only difference between \mathcal{O} and \mathcal{N} is the edge-coloration of four edges (namely, the central (12)-bicolored bubble adjacent to μ_0 and ν_0), whence the following connected sum is well-defined:

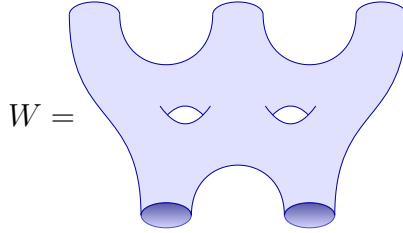
$$G((\epsilon_1, \iota_1), \dots, (\epsilon_m, \iota_m)) = \mathcal{S}(\epsilon_1, \iota_1) \#_{\mu_0^1 \nu_0^2} \mathcal{S}(\epsilon_2, \iota_2) \#_{\mu_0^2 \nu_0^3} \dots \#_{\mu_0^{m-1} \nu_0^m} \mathcal{S}(\epsilon_m, \iota_m) \dots$$

where μ_0^i refers to the μ_0 edge of $\mathcal{P}(\epsilon_i)$ and ν_0^i has similar notation. Define then the graph $\mathcal{Q}_{g,B,C}$ by evaluating $G((\epsilon_1, \iota_1), \dots, (\epsilon_m, \iota_m))$ at

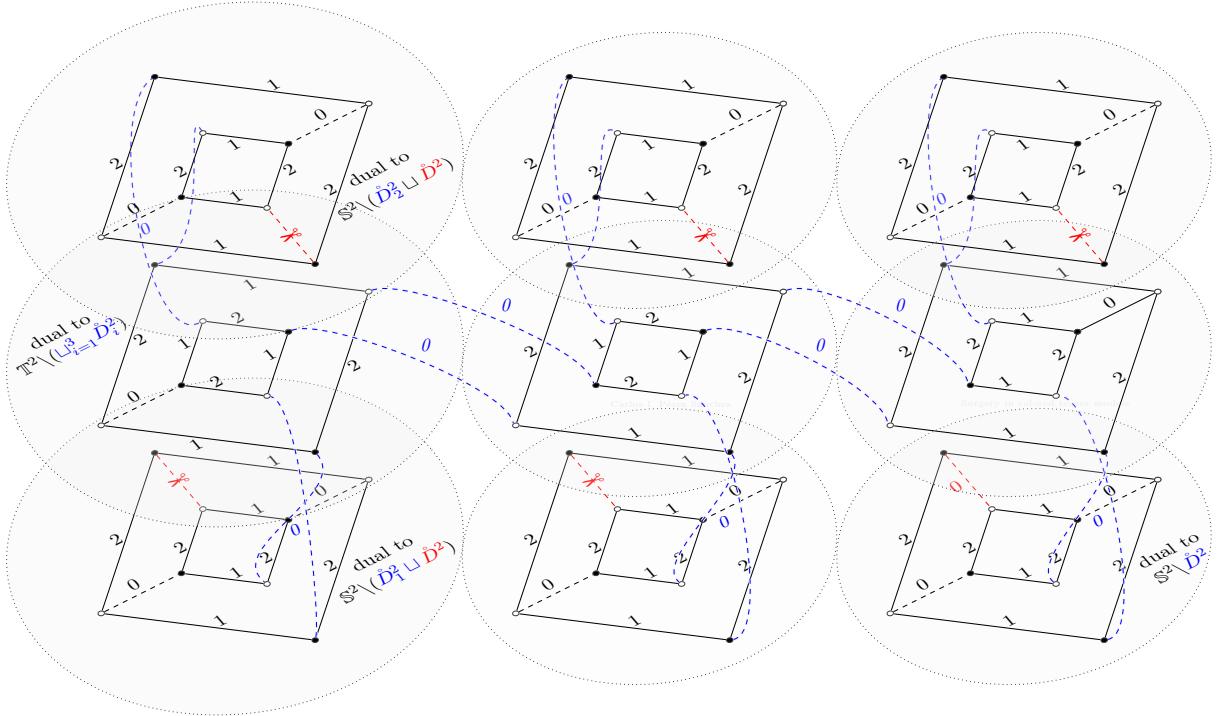
$$\epsilon_k = \begin{cases} 1 & \text{if } 1 \leq k \leq g, \\ 0 & \text{if } k > g, \end{cases} \quad \text{and} \quad \iota_k = \begin{cases} 2 & \text{if } 1 \leq k \leq B, \\ 1 & \text{if } B < k \leq C, \\ 0 & \text{if } k > C. \end{cases}$$

Each 0-colored-edge removal creates exactly a boundary component \mathbb{S}^1 , for none of the 2-bubbles of α_0 and β_0 implies the edges μ_0 and ν_0 . Hence one has indeed created $C + B$ \mathbb{S}^1 -boundaries. If we cap them (closing all the broken α_0 and β_0) we get $\mathcal{Q}_{g,0,0}$ which is the \mathcal{Q}_g of Lemma 3.6 and hence has genus g . \square

Example 3.11. Consider the following genus-2 bordism $W : \sqcup^3 \mathbb{S}^1 \rightarrow \sqcup^2 \mathbb{S}^1 \in 2\text{-Cob}$,



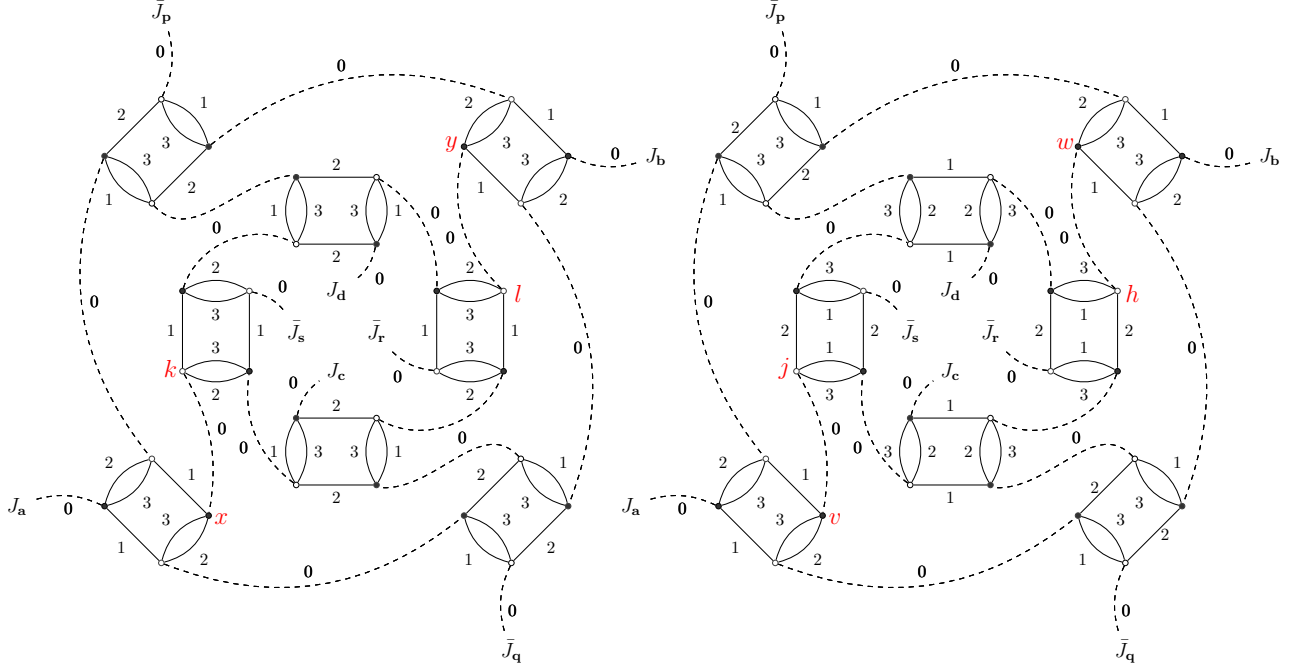
The construction for $\mathcal{Q}_{2,2,3}$ is, explicitly, the following graph, in which we represented by \asymp the opening of the 0-colored edges:



The theorem states that $\mathcal{Q}_{2,2,3} \in \mathfrak{Feyn}_2((\varphi\bar{\varphi}^2))$ triangulates W .

4. THE BOUNDARY SECTOR OF THE φ_3^4 -THEORY

4.1. Completeness of the boundary sector. Let $\mathfrak{Feyn}_3(\varphi^4)$ be (shorthand for) the set of connected Feynman graphs of the rank-3 φ^4 -colored tensor theory with the three vertices (2.8). Ribb is the set of connected ribbon graphs and $\text{Riem}_{c,cl,o}$ the set of



(A) This graph defines \mathcal{M}_0 . Its boundary is the ribbon graph \mathcal{R}_0 . (B) By definition, this graph is \mathcal{M}_1 . Its boundary is found to be \mathcal{R}_1 .

FIGURE 4. These are the two φ_3^4 -graphs whose boundary are, respectively, (a ribbon graph on) the sphere and torus given by eq. (2.11). (The vertex-labels j, h, \dots, x, y assist in a proof below.)

homeomorphism-classes of closed orientable *connected* Riemannian surfaces, $\text{Riem}_{c,\text{cl},o} \simeq \mathbb{N}_0$.

Proposition 4.1. *In the rank-3 φ^4 -model, for each integer $g \geq 0$, there exists (at least) one Feynman graph whose boundary is (a triangulation of) the closed orientable surface of genus g . That is, the following map is surjective,*

$$\beta : \mathfrak{Feyn}_3(\varphi^4)_{c.b.} \xrightarrow{\partial} \text{Ribb} \xrightarrow{\Delta} \text{Riem}_{c,\text{cl},o},$$

where $\mathfrak{Feyn}_3(\varphi^4)_{c.b.}$ consist of the graphs in $\mathfrak{Feyn}_3(\varphi^4)$ with connected boundary.

To prove this proposition we need the following lemma.

Lemma 4.2. *There are graphs in $\mathfrak{Feyn}_3(\varphi^4)$ triangulating \mathbb{S}^2 and \mathbb{T}^2 .*

Proof. Exclusively using the three vertices \mathcal{V}_i of the φ_3^4 -theory, we construct graphs \mathcal{M}_0 and \mathcal{M}_1 whose boundaries are ribbon graphs which represent, respectively, the sphere and the torus. The first might be done trivially by coning any of the vertices of the theory, \mathcal{V}_i , and construct the CW-complex to it, but we prefer to construct a particular graph \mathcal{M}_0 which will be useful later. The wished graphs are defined in Figure 4 and their boundaries are computed straightforwardly from Definition 2.12:

$$\partial\mathcal{M}_0 = \mathcal{R}_0 \quad \text{and} \quad \partial\mathcal{M}_1 = \mathcal{R}_1.$$

where \mathcal{R}_0 and \mathcal{R}_1 are given in Example 2.7. Then $\Delta \circ \partial(\mathcal{M}_0) \simeq \mathbb{S}^2$, $\Delta \circ \partial(\mathcal{M}_1) \simeq \mathbb{T}^2$. \square

Proof of Proposition 4.1. From \mathcal{M}_1 we can cut the color-0 edge \overline{jv} from j to v , and the edge \overline{hw} between h and w , resulting in the graph $\mathcal{M}_1(j, h; v, w)$ with four additional external legs at said vertices. Similarly, denote by $\mathcal{M}_0(k, l; x, y)$ the graph obtained from

\mathcal{M}_0 by deletion of the color-0 edges \overline{kx} and \overline{ly} . We will see that \mathcal{M}_1 strategically glued with two copies of \mathcal{M}_0 becomes handy. Define then the graphs \mathcal{T}_0 and \mathcal{T}_1 through

$$\mathcal{T}_0^\vee(k_1, l_2; x_1, y_2) := \mathcal{M}_0^\vee(k_1, l_1; x_1, y_1) \underbrace{\mathcal{M}_0^\vee(j, h; v, w)}_{\text{glued}} \mathcal{M}_0^\vee(k_2, l_2; x_2, y_2), \quad (4.1)$$

and

$$\mathcal{T}_1^\vee(k_1, l_2; x_1, y_2) := \mathcal{M}_0^\vee(k_1, l_1; x_1, y_1) \underbrace{\mathcal{M}_1^\vee(j, h; v, w)}_{\text{glued}} \mathcal{M}_0^\vee(k_2, l_2; x_2, y_2). \quad (4.2)$$

For sake of clarity, we display the last one of these contractions in Figure 5. With this notation, eqs. (4.1) and (4.2) are conveniently shortened as $\mathcal{T}_\alpha = (\mathcal{M}_0)_e \#_E (\mathcal{M}_\alpha)_F \#_f (\mathcal{M}_0)$ for $\alpha = 0, 1$, where $e = \overline{l_1 y_1}$, $E = \overline{hw}$, $F = \overline{jv}$ and $f = \overline{k_2 x_2}$. For integers $g \geq 2$ we take g copies $\mathcal{T}_1^{(1)}, \dots, \mathcal{T}_1^{(g)}$ of \mathcal{T}_1 and denote by h_r the edge $\overline{k_1 x_1}$ in the r -th copy $\mathcal{T}_1^{(r)}$; likewise denote by i_r the edge $\overline{l_2 y_2}$ in $\mathcal{T}_1^{(r)}$. We now set

$$\mathcal{T}_g := (\mathcal{T}_1^{(1)})_{h_1} \#_{i_2} (\mathcal{T}_1^{(2)})_{h_2} \#_{i_3} \cdots \#_{h_{g-1}} (\mathcal{T}_1^{(g)})_{i_g} \quad (4.3)$$

and claim that $\beta \mathcal{T}_g \simeq \Sigma^g$. Indeed, notice first that the boundary graph of \mathcal{T}_1 is the graph \mathcal{O} in Figure 6, which triangulates a torus. By construction, $\partial \mathcal{T}_g$ is putting together g copies of \mathcal{O} , as described in Remark 3.7, such that $\partial \mathcal{T}_g = \mathcal{K}_g$. Again by Remark 3.7, this implies that $\Delta \circ \partial \mathcal{T}_g = \Delta \mathcal{K}_g$ is homeomorphic to Σ^g . \square

Remark 4.3. Actually, a slightly more general result holds, but we remark first that as consequence of the last proposition, the set $\mathbf{T} = \{\mathcal{T}_0, \mathcal{T}_1, \mathcal{T}_2, \dots\} \subset \mathfrak{Fenn}_3(\varphi^4)$ endowed with the contraction $\#$ is a monoid. Moreover, the restriction of $\beta|_{\mathbf{T}}$ to that set is a monoid-morphism

$$(\mathbf{T}, \#) \rightarrow (\text{Riem}_{\text{c,cl,o}}, \#).$$

The associativity is obvious. In this claim, the marked edges at \mathcal{T}_g are given by i_1 and h_g in eq. (4.3). From now on, we take this as convention. The neutral elements of \mathbf{T} and $\text{Riem}_{\text{c,cl,o}}$ are \mathcal{T}_0 and \mathbb{S}^2 , respectively.

Lemma 4.4. *The following graphs $\mathcal{S}_1, \mathcal{S}_2 \in \mathfrak{Fenn}_3(\varphi^4)$ separate boundary components:*

$$\mathcal{S}_1(a, b; p, q) := \begin{array}{c} \begin{array}{ccccccc} & & 2 & & 3 & & 1 \\ & \text{---} & \text{---} & \text{---} & \text{---} & \text{---} & \text{---} \\ p & 0 & \bullet & 0 & \bullet & 0 & \bullet & 0 & b \\ & \text{---} & \text{---} & \text{---} & \text{---} & \text{---} & \text{---} \\ & 1 & \text{---} & 1 & 2 & \text{---} & 3 \\ & \text{---} & \text{---} & \text{---} & \text{---} & \text{---} & \text{---} \\ a & 0 & \bullet & 0 & \bullet & 0 & \bullet & 0 \\ & \text{---} & \text{---} & \text{---} & \text{---} & \text{---} & \text{---} \\ & & 2 & & 3 & & 1 \end{array} \end{array} \quad (4.4)$$

$$\mathcal{S}_2(a, b; p, q) := \begin{array}{c} \begin{array}{ccccccc} & & 0 & & 0 & & 0 \\ & \text{---} & \text{---} & \text{---} & \text{---} & \text{---} & \text{---} \\ a & 0 & \bullet & 0 & \bullet & 0 & \bullet & 0 & q \\ & \text{---} & \text{---} & \text{---} & \text{---} & \text{---} & \text{---} \\ & 1 & \text{---} & 2 & \text{---} & 2 & \text{---} & 3 \\ & \text{---} & \text{---} & \text{---} & \text{---} & \text{---} & \text{---} \\ p & 0 & \bullet & 0 & \bullet & 0 & \bullet & 0 & b \\ & \text{---} & \text{---} & \text{---} & \text{---} & \text{---} & \text{---} \\ & 2 & \text{---} & 3 & 2 & \text{---} & 3 \\ & \text{---} & \text{---} & \text{---} & \text{---} & \text{---} & \text{---} \\ & & 1 & & 1 & & 3 \end{array} \end{array} \quad (4.5)$$

To be precise, given two open graphs $\mathcal{G}_1, \mathcal{G}_2 \in \mathfrak{Fenn}_3(\varphi^4)$, with $2p_1$ and $2p_2$ external legs respectively

$$\mathcal{G}_1(c^{(1)}, c^{(2)}, \dots, c^{(p_1)}; r^{(1)}, r^{(2)}, \dots, r^{(p_1)}) \quad \text{and} \quad \mathcal{G}_2(d^{(1)}, d^{(2)}, \dots, d^{(p_2)}; s^{(1)}, s^{(2)}, \dots, s^{(p_2)})$$

for $\alpha = 1, 2$ and for any $1 \leq i, j \leq p_1$ and $1 \leq k, l \leq p_2$, the contraction

$$\mathcal{C}_\alpha = \mathcal{G}_1(\dots, \underbrace{c^{(i)}, \dots, r^{(j)}}_{\text{glued}}, \dots) \mathcal{S}_\alpha(a, b; p, q) \underbrace{\mathcal{G}_2(\dots, d^{(k)}, \dots, s^{(l)}, \dots)}_{\text{glued}}$$

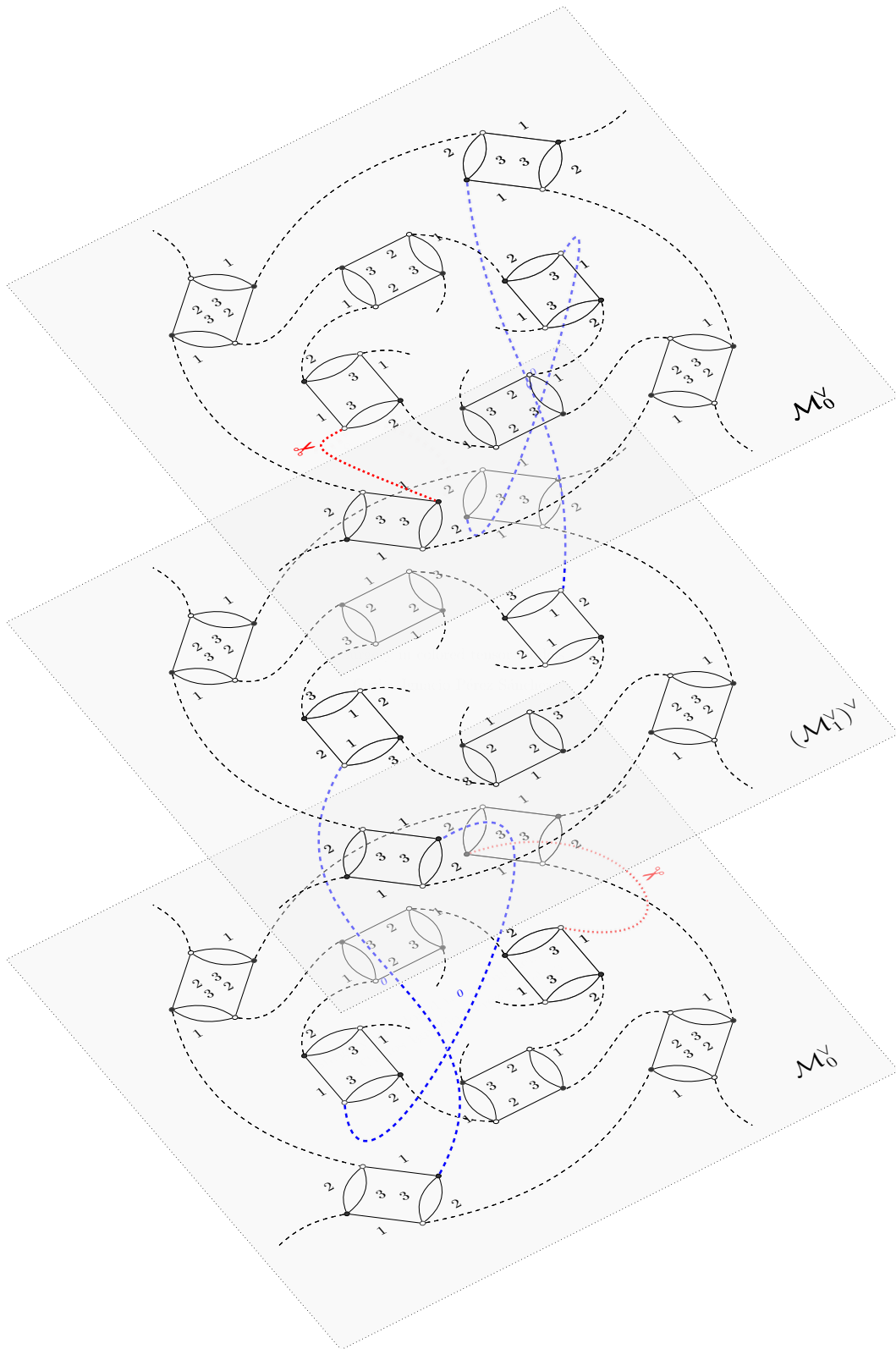


FIGURE 5. This is the building block of our construction. To avoid a prolixity, we omitted here the 0-color labels. All dotted labels are either external lines or Wick contractions. The thick lines between the planes are the Wick contractions referred to in eq. (4.2). Edges marked with \asymp are then opened and glued with another block.

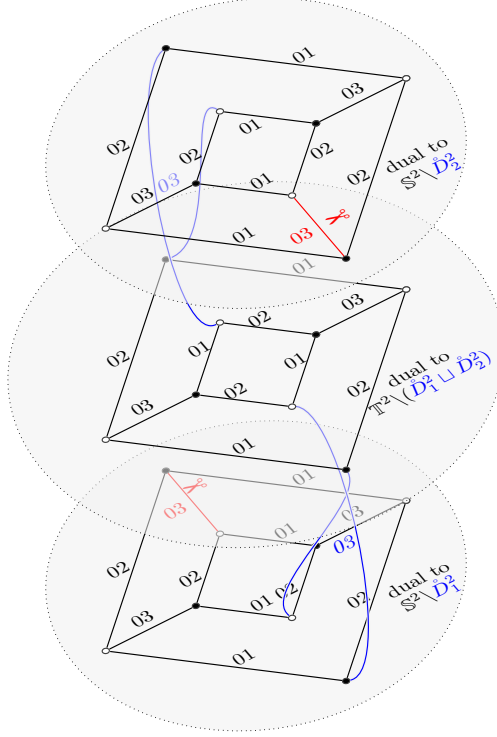


FIGURE 6. The boundary graph of the graph in Figure 5.

yields a graph \mathcal{C}_α , whose boundary is

$$\partial(\mathcal{G}_1(c^{(1)}, \dots, \overline{c^{(i)}, \dots}; r^{(1)}, \dots, r^{(j)}, \dots)) \sqcup \partial(\mathcal{G}_2(d^{(1)}, \dots, \overline{d^{(k)}, \dots}; s^{(1)}, \dots, s^{(l)}, \dots)). \quad (4.6)$$

The content of this result can be easier to visualize with if we represent \mathcal{C}_α as



where the dots summarize the remaining edges (which of them remain uncontracted is, according to the proposition, irrelevant). Hence Lemma 4.4 says that

$$\partial\mathcal{C}_\alpha = \partial \left(\begin{array}{c} \vdots \\ \text{---} \text{---} \text{---} \\ \text{---} \text{---} \text{---} \\ \text{---} \text{---} \text{---} \\ \vdots \end{array} \right) \sqcup \partial \left(\begin{array}{c} \text{---} \text{---} \text{---} \\ \text{---} \text{---} \text{---} \\ \text{---} \text{---} \text{---} \\ \text{---} \text{---} \text{---} \\ \vdots \end{array} \right)$$

Proof. Let \mathcal{K} be the graph in (4.6). We verify that the edge and vertex sets of both \mathcal{K} and $\partial\mathcal{C}_\alpha$ are the same.

- *Vertices.* $\partial\mathcal{C}_\alpha$ has $2(p_1 + p_2 - 2)$ vertices, out of which $2(p_\nu - 1)$ correspond to the remaining external lines of \mathcal{G}_ν ($\nu = 1, 2$) still attached to \mathcal{G}_ν . Also $\mathcal{K}^{(0)} = 2(p_1 + p_2 - 2)$. Moreover, by mere definition, $(\partial\mathcal{C}_\alpha)^{(0)}$ and $\mathcal{K}^{(0)}$ have the same bipartiteness, whence they are equal as vertex-sets of a bipartite graph.
- *Edges.* Here we exclude first the case in which $p_1 = p_2 = 1$. If that happens, we have trivially $\partial\mathcal{C}_\alpha = \emptyset = \mathcal{K}_\alpha$. Assume then that $\partial\mathcal{C}_\alpha \neq \emptyset$ and choose an arbitrary color $\ell = 1, 2, 3$. Note first that any edge in $\partial\mathcal{C}_\alpha$ that does not touch \mathcal{S}_α , is trivially in \mathcal{K}_α and vice versa. Let then $e_\ell \in (\partial\mathcal{C}_\alpha)_e^{(1)}$ intersect \mathcal{S}_α . Then e_ℓ corresponds

to a $(0e)$ -colored path in \mathcal{C}_α connecting a white vertex with a black one, which in this case means that a $(0e)$ -colored path connects either⁴

- (i) $c = c^{(n)}$ ($n \neq i$) with $r = r^{(m)}$ ($m \neq j$),
- (ii) $c = c^{(n)}$ ($n \neq i$) with $s = s^{(m)}$ ($m \neq l$),
- (iii) $d = d^{(n)}$ ($n \neq k$) with $s = s^{(m)}$ ($m \neq l$), or
- (iv) $d = d^{(n)}$ ($n \neq k$) with $r = r^{(m)}$ ($m \neq j$).

Since the only $(0e)$ -colored paths in \mathcal{S}_α connect either a with p or b with q , there is no path from c to s , whence (ii) is false. Similarly, (iv) cannot hold either. This leaves us with cases (i) and (iii). Since the latter is obtained mutatis mutandis from (i), we only analyze (i). We assume w.l.o.g. that $p_1 \neq 1$ (otherwise, by assumption $p_2 \neq 1$ and in that case we would be left with the third case). Now, (i) holds if and only if the restriction $e_\ell|_{\mathcal{S}_\alpha}$ of e_ℓ to \mathcal{S}_α is $(0e)$ -bicolored, in which case, e_ℓ enters \mathcal{S}_α through p and exits through a . This happens iff c connects r by replacing that restriction $e_\ell|_{\mathcal{S}_\alpha}$ by a 0 line connecting a with p , that is iff $e_\ell \in \mathcal{K}_\ell^{(1)}$. We conclude $(\partial\mathcal{C}_\alpha)_\ell^{(1)} = \mathcal{K}_\ell^{(1)}$, and since ℓ is arbitrary, $(\partial\mathcal{C}_\alpha)^{(1)} = \mathcal{K}^{(1)}$. \square

It is trivial to construct Feynman graphs \mathcal{G} which have disconnected boundary, just by letting \mathcal{G} itself be disconnected. This would be rather useless, though, for \mathcal{G} would be cancelled out in the generating functional of connected correlation functions. The previous lemma says that, nevertheless, it is possible to ‘separate boundaries’ at wish. Moreover, it tells us how to generate *connected* graphs with a precise disconnected boundary. This can be reformulated as follows:

Proposition 4.5. *If $\mathcal{F}, \mathcal{G} \in \mathfrak{Feyn}_3(\varphi^4)$ both have at least one internal 0-colored edge, $f \in \text{inn}(\mathcal{F}_0^{(1)})$ and $g \in \text{inn}(\mathcal{G}_0^{(1)})$ (i.e. none of the \mathcal{F}_i is the cone of a graph). Then $\mathcal{F}_f \#_k (\mathcal{P}_\alpha)_l \#_g \mathcal{G} \in \mathfrak{Feyn}_3(\varphi^4)$ and*

$$\partial(\mathcal{F}_f \#_k (\mathcal{P}_\alpha)_l \#_g \mathcal{G}) = \partial\mathcal{F} \sqcup \partial\mathcal{G},$$

where $\mathcal{P}_\alpha = \mathcal{S}_\alpha(\overbrace{a, b; p, q}^{\text{---}})$ and $k = \overline{ap}$ and $l = \overline{bq}$, and $\alpha = 1, 2$.

Proof. Notice that

$$\mathcal{F}_f \#_k (\mathcal{P}_\alpha)_l \#_g \mathcal{G} = \mathcal{F}^\vee(s(f), t(f)) \underbrace{\mathcal{S}_\alpha(a, b; p, q)}_{\text{---}} \overbrace{\mathcal{G}^\vee(s(g), t(g))}^{\text{---}}.$$

Then the result follows by applying Lemma 4.4 to this graph. The graph in question is in $\mathfrak{Feyn}_3(\varphi^4)$ because so are \mathcal{F} , \mathcal{G} and \mathcal{S}_α . \square

The next statement is the actual utilization of Lemma 4.4 and Proposition 4.5.

Theorem 4.6. *Let $\text{Riem}_{\text{cl},o}$ be the set of (possibly disconnected) closed, orientable Riemannian surfaces. Then the map γ*

$$\gamma = \Delta \circ \partial : \mathfrak{Feyn}_3(\varphi^4) \xrightarrow{\partial} \text{IRibb} \xrightarrow{\Delta} \text{Riem}_{\text{cl},o}$$

is surjective. Here IRibb is the set of possibly disconnected ribbon graphs.

Proof. Let $M \in \text{Riem}_{\text{cl},o}$. If $\Sigma^g = \#_{i=1}^g \mathbb{T}^2$, M has the general form

$$M \simeq (\mathbb{S}^2)^{\sqcup b_0} \sqcup (\mathbb{T}^2)^{\sqcup b_1} \sqcup (\mathbb{T}^2 \# \mathbb{T}^2)^{\sqcup b_2} \dots = \sqcup_{g=0}^m (\Sigma^g)^{\sqcup b_g}, \quad (b_0, \dots, b_m, m \in \mathbb{Z}_{\geq 0}) \quad (4.7)$$

being $(\Sigma^g)^{\sqcup n}$ the n -fold disjoint union $\Sigma^g \sqcup \dots \sqcup \Sigma^g$. The case $m = 0$ is trivial, for the empty manifold $M = \emptyset$ can be obtained as boundary of any closed graph, so we assume

⁴We transfer the labels of the external lines to the vertices of the boundary graphs.

$m > 0$. We construct a graph \mathcal{G} with $(\Delta \circ \partial)\mathcal{G} \simeq M$. From Proposition 4.1 we can construct the independent pieces Σ^g for arbitrary genus g . Then, we use Proposition 4.5 to produce the desired disjoint sums. Define

$$R_{[b_0, b_1, \dots, b_m]} := (\#^{b_0}(\mathcal{T}_0 \# \mathcal{P}_\alpha)) \# (\#^{b_1}(\mathcal{T}_1 \# \mathcal{P}_\alpha)) \# (\#^{b_2}(\mathcal{T}_2 \# \mathcal{P}_\alpha)) \# \dots \# (\#^{b_{m-1}}(\mathcal{T}_{m-1} \# \mathcal{P}_\alpha) \# \mathcal{T}_m).$$

To keep a simple notation, the edges have been suppressed. The edges of each copy of \mathcal{T}_g implied in each operation $\#$ are specified by remark 4.3, and those of each copy of the graph \mathcal{P}_α are the edges k and l given in Proposition 4.5. We claim that $\gamma(R_{[b_0, b_1, \dots, b_m]}) \simeq M$. First, we rewrite $R_{[b_0, b_1, \dots, b_m]}$ in terms of simpler pieces as

$$U_j^{(b_j)} := \mathcal{T}_j \# \mathcal{P}_\alpha \# \dots \# \mathcal{P}_\alpha \# \mathcal{T}_j \quad (j = 0, \dots, m),$$

where \mathcal{T}_j appears b_j times and \mathcal{P}_α precisely $b_j - 1$ times. One has then $R_{[b_0, b_1, \dots, b_m]} = U_0^{(b_0)} \# \mathcal{P}_\alpha \# \dots \# \mathcal{P}_\alpha \# U_m^{(b_m)}$. Now, by Proposition 4.5, the boundary of this graph is given by $\partial R_{[b_0, b_1, \dots, b_m]} = \partial U_0^{(b_0)} \sqcup \partial U_1^{(b_1)} \dots \sqcup \partial U_m^{(b_m)}$. Notice that for any $j = 0, \dots, m$, that very proposition can be used again to get $\partial U_j^{(b_j)} = \sqcup_{i=1}^{b_j} \partial \mathcal{T}_j$. Applying Δ to this expression one has $\Delta \circ \partial U_j^{(b_j)} = \sqcup_{i=1}^{b_j} \beta \mathcal{T}_j \simeq (\Sigma^j)^{\sqcup b_j}$, by Proposition 4.1. Thus

$$\gamma(R_{[b_0, b_1, \dots, b_m]}) = \Delta \circ \partial U_1^{(b_1)} \sqcup \Delta \circ \partial U_2^{(b_2)} \dots \Delta \circ \partial U_m^{(b_m)} \simeq \sqcup_{g=0}^m (\Sigma^g)^{\sqcup b_g} = M. \quad \square$$

5. CONCLUSIONS

We defined the connected sum of 3-colored graphs and used it to prove the surjectivity of the map ξ in the following commuting diagram:

$$\begin{array}{ccc} & \mathfrak{F}\mathfrak{e}\mathfrak{h}\mathfrak{n}_2((\varphi\bar{\varphi})^2) & \\ \swarrow & & \searrow \xi \\ \sqcup_{k=0}^\infty \mathbf{Grph}_{\text{col}, 2+1}^{(2k)} & \xrightarrow{\Delta} & \mathbf{2-Cob} \end{array} \quad (5.1)$$

Tangentially, this might provide some link between the rank-2 tensor models and Atiyah's Topological Quantum Field Theories [2], where one studies functors from $\mathbf{2-Cob}$ to the category of Hilbert spaces. case of (5.1) is γ in the following commutative diagram:

$$\begin{array}{ccc} & \mathfrak{F}\mathfrak{e}\mathfrak{h}\mathfrak{n}_2((\varphi\bar{\varphi})^2) & \\ \swarrow & & \searrow \gamma \\ \mathbf{Grph}_{\text{col}, 2+1} & \xrightarrow{\Delta} & \mathbf{Riem}_{\text{c}, \text{cl}, \text{o}} \end{array} \quad (5.2)$$

Trivially, CTM-graphs that represent a (sub)category of boundaryless manifolds (here $\mathbf{Riem}_{\text{c}, \text{cl}, \text{o}}$) can be exhibited as null-bordant, by just coning each graph. The non trivial part is showing that, in this case, any surface in $\mathbf{Riem}_{\text{c}, \text{cl}, \text{o}}$ is null-bordant via a suitable graph in $\mathfrak{F}\mathfrak{e}\mathfrak{h}\mathfrak{n}_3(\varphi^4)$, which we constructed. Moreover, any two surfaces in $\mathbf{Riem}_{\text{cl}, \text{o}}$ (even disconnected) are also cobordant in the sense of the φ_3^4 -theory:

$$\begin{array}{ccc} & \mathfrak{F}\mathfrak{e}\mathfrak{h}\mathfrak{n}_3(\varphi^4) & \\ \swarrow \partial & & \searrow \gamma \\ \mathbf{IIGrph}_{\text{col}, 3} & \xrightarrow{\Delta} & \mathbf{Riem}_{\text{cl}, \text{o}} \end{array} \quad (5.3)$$

It remains to generalize the connected sum of graphs in $\mathbf{Grph}_{\text{col}, d}$ for $d > 3$. But, in the near future, we would like to apply results obtained here. An immediate consequence concerns the non-perturbative [33] treatment of the Ward Identity for rank-3 tensor models

[32, 38]. In order to undertake that problem, one needs the expansion of the free energy $\log Z[J, \bar{J}]$ in boundary graphs, analogous to in the matrix model case [19, Sec. 2.3].

The fact that the boundary sector $\partial\mathfrak{Fen}_3(\varphi^4)$, as proven here, generates all of $\text{Riem}_{\text{cl},0}$ facilitates our Ansatz regarding this expansion. There the divergence degree of graphs can be expressed in terms of certain integer-valued function $\tilde{\omega}$ on $\text{Grph}_{\text{col},D+1}^{(2k)}$ (for any $k \in \mathbb{N}$) that extends Gurău’s degree ω . The integer $\tilde{\omega}(\mathcal{G})$ is given in terms of the so called pinched jackets of \mathcal{G} . For us, it is important that the genus and Gurău’s degree are the same for 3-colored graphs. One has then for $\mathcal{G} \in \text{Grph}_{\text{col},3}^{(2k)}$, $\tilde{\omega}(\mathcal{G}) \geq 3 \cdot \omega(\partial\mathcal{G}) = 3 \sum_{\mathcal{R} \subset \partial\mathcal{G}} g(\mathcal{R})$, summing⁸ over the the connected components of the boundary graph $\partial\mathcal{G}$. The present work helps to compute the boundary graph $\partial\mathcal{G}$, and hence to bound the degree $\tilde{\omega}(\mathcal{G})$.

In [33] it will be proven that the correlation functions $G_{\mathcal{B}}$ of the φ_3^4 -model are indexed by boundary graphs $\mathcal{B} \in \partial\mathfrak{Fen}_3(\varphi^4)$. It will be useful to expand these functions in Gurău’s degree, as done in the matrix theory-formulation of the ($\Omega = 1$)-Grosse-Wulkenhaar φ^4 -model [19] in terms of the genus. In there, using such expansion, combined with the a full Ward identity and the Schwinger-Dyson equations yielded a closed equations for correlation functions and that techniques will be extended to the present setting.

As another immediate application, the natural continuation of this work is to relax some of the symmetry and to pose Question (\star) in the framework of multi-orientable [41] or $O(N)$ -tensor models [11].

A second, quite different application is the addition of bosonic fields. In dimension two, for instance, using Theorem 3.10 and constructs before it, one has control of the gluings’ topology, even of those made of a large number of interaction vertices. This can both ease computations and be reused define gauge theories on (computable) random spaces. An approach is, first, to adapt the gauge theory on usual graphs à la Baez [3] to our colored graphs. Secondly, one would add gauge fields à la Marcolli-van Suijlekom [26] using representation of graphs (here tensor-model Feynman graphs used as random-‘manifold base’) in the category of finite dimensional spectral triples with vanishing Dirac operator. In that respect, the connection between noncommutative geometry and matrix models would be based on recent results by Barrett and Glaser [4], which treat the *quantum* Connes-Chamseddine spectral action [12, 13] as a certain matrix model.

ACKNOWLEDGEMENT

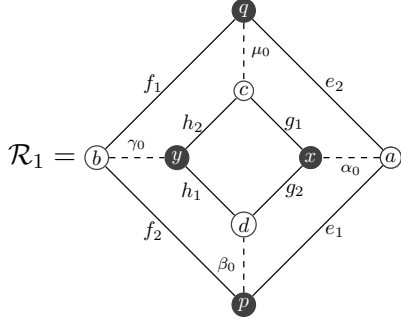
The author wishes to thank:

- The *Deutscher Akademischer Austauschdienst* (DAAD) mainly, but also the *Sonderforschungsbereich 878* “Groups, Geometry & Actions” (SFB 878), for financial support.
- Joseph Ben Geloun, Raimar Wulkenhaar and Adrian Tanasă for useful comments.
- The Erwin Schrödinger International Institute for Mathematical Physics, Vienna, for hospitality during the ESI-Program “The interrelation between mathematical physics, number theory and non-commutative geometry”.

⁸The inequality has been proven in [6, Lemma 4] (see also [39, Cor. B4]); for the equality, see here Example 2.7.

APPENDIX A. COMPUTING HOMOLOGY OF COLORED GRAPHS

Example A.1. To compute its bubble-homology, as proposed in Ex. 2.7 one chooses an (ordered) basis for each dimension according to following labels:



$$\begin{aligned} C_0(\mathcal{R}_1) &= \langle a, b, c, d, p, q, x, y \rangle_{\mathbb{Z}}, \\ C_1(\mathcal{R}_1) &= \langle e_1, e_2, f_1, f_2, g_1, g_2, h_1, h_2, \alpha_0, \beta_0, \gamma_0, \mu_0 \rangle_{\mathbb{Z}}, \\ C_2(\mathcal{R}_1) &= \langle \mathcal{B}^{01}, \mathcal{B}^{02}, \mathcal{B}_{\text{outside}}^{12}, \mathcal{B}_{\text{inside}}^{12} \rangle_{\mathbb{Z}}. \end{aligned}$$

In the chain complex $0 \rightarrow \mathbb{Z}^4 \simeq C_2(\mathcal{R}_1) \xrightarrow{\partial_2} \mathbb{Z}^{12} \simeq C_1(\mathcal{R}_1) \xrightarrow{\partial_1} C_0(\mathcal{R}_1) \simeq \mathbb{Z}^8 \rightarrow 0$ the non-trivial boundary operators are, in the chosen bases, given by:

$$\partial_1 = \begin{pmatrix} -1 & -1 & 0 & 0 & 0 & 0 & 0 & 0 & -1 & 0 & 0 & 0 \\ 0 & 0 & -1 & -1 & 0 & 0 & 0 & 0 & 0 & 0 & -1 & 0 \\ 0 & 0 & 0 & 0 & -1 & 0 & 0 & -1 & 0 & 0 & 0 & -1 \\ 0 & 0 & 0 & 0 & 0 & -1 & -1 & 0 & 0 & -1 & 0 & 0 \\ 1 & 0 & 0 & 1 & 0 & 0 & 0 & 0 & 0 & 1 & 0 & 0 \\ 0 & 1 & 1 & 0 & 0 & 0 & 0 & 0 & 0 & 0 & 0 & 1 \\ 0 & 0 & 0 & 0 & 1 & 1 & 0 & 0 & 1 & 0 & 0 & 0 \\ 0 & 0 & 0 & 0 & 0 & 0 & 1 & 1 & 0 & 0 & 1 & 0 \end{pmatrix} \sim \begin{pmatrix} 1 & 0 & 0 & 1 & 0 & 0 & 0 & 0 & 0 & 1 & 0 & 0 \\ 0 & 1 & 0 & -1 & 0 & 0 & 0 & 0 & 0 & 0 & -1 & 1 \\ 0 & 0 & 1 & 1 & 0 & 0 & 0 & 0 & 0 & 0 & 1 & 0 \\ 0 & 0 & 0 & 1 & 0 & 0 & 1 & 0 & 0 & 0 & 0 & 1 \\ 0 & 0 & 0 & 0 & 1 & 0 & -1 & 0 & 1 & 0 & -1 & 0 \\ 0 & 0 & 0 & 0 & 0 & 1 & 0 & 0 & 1 & 0 & 1 & 0 \\ 0 & 0 & 0 & 0 & 0 & 0 & 0 & 1 & -1 & 1 & -1 & 0 \\ 0 & 0 & 0 & 0 & 0 & 0 & 0 & 0 & 0 & 0 & 0 & 0 \end{pmatrix}$$

and

$$\partial_2 = \begin{pmatrix} 1 & 0 & -1 & 0 \\ 0 & 1 & 1 & 0 \\ 1 & 0 & -1 & 0 \\ 0 & 1 & 1 & 0 \\ 1 & 0 & 0 & -1 \\ 0 & 1 & 0 & 1 \\ 1 & 0 & 0 & -1 \\ 0 & 1 & 0 & 1 \\ -1 & -1 & 0 & 0 \\ -1 & -1 & 0 & 0 \\ -1 & -1 & 0 & 0 \\ -1 & -1 & 0 & 0 \end{pmatrix} \sim \begin{pmatrix} 1 & 0 & 0 & 0 \\ 0 & 1 & 0 & 0 \\ 1 & 0 & 0 & 0 \\ 0 & 1 & 0 & 0 \\ 0 & 0 & 1 & 0 \\ 1 & 1 & -1 & 0 \\ 0 & 0 & 1 & 0 \\ 1 & 1 & -1 & 0 \\ -1 & -1 & 0 & 0 \\ -1 & -1 & 0 & 0 \\ -1 & -1 & 0 & 0 \\ -1 & -1 & 0 & 0 \end{pmatrix},$$

where the tilde means a change of basis, which in each case leads to row or column reduction. Since $\partial_3 = 0$, $H_2(\mathcal{R}_1) = \ker \partial_2 = \mathbb{Z}$. On the other hand the column reduction of ∂_1 is

$$\partial_1 M = \begin{pmatrix} 1 & 0 & 0 & 0 & 0 & 0 & 0 & 0 & 0 & 0 & 0 & 0 \\ 0 & 1 & 0 & 0 & 0 & 0 & 0 & 0 & 0 & 0 & 0 & 0 \\ 0 & 0 & 1 & 0 & 0 & 0 & 0 & 0 & 0 & 0 & 0 & 0 \\ 0 & 0 & 0 & 1 & 0 & 0 & 0 & 0 & 0 & 0 & 0 & 0 \\ 0 & 0 & 0 & 0 & 1 & 0 & 0 & 0 & 0 & 0 & 0 & 0 \\ 0 & 0 & 0 & 0 & 0 & 1 & 0 & 0 & 0 & 0 & 0 & 0 \\ 0 & 0 & 0 & 0 & 0 & 0 & 1 & 0 & 0 & 0 & 0 & 0 \\ -1 & -1 & -1 & -1 & -1 & -1 & -1 & -1 & 0 & 0 & 0 & 0 \end{pmatrix}$$

where

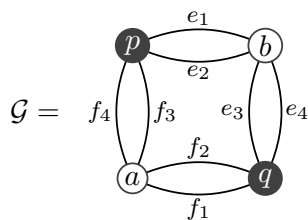
$$M = \begin{pmatrix} 0 & 0 & 0 & 0 & 1 & 0 & 0 & 0 & -1 & -1 & 0 & 0 \\ 0 & 1 & 0 & 0 & 0 & 1 & 0 & 0 & 1 & 0 & 1 & -1 \\ 0 & -1 & 0 & 0 & 0 & 0 & 0 & 0 & -1 & 0 & -1 & 0 \\ 0 & 0 & 0 & 0 & 0 & 0 & 0 & 0 & 1 & 0 & 0 & 0 \\ 0 & 0 & -1 & 0 & 0 & 0 & 0 & -1 & 0 & 0 & 0 & -1 \\ 1 & 1 & 1 & 0 & 1 & 1 & 1 & 1 & 0 & -1 & 1 & 0 \\ -1 & -1 & -1 & -1 & -1 & -1 & -1 & -1 & 0 & 0 & -1 & 0 \\ 0 & 0 & 0 & 0 & 0 & 0 & 0 & 1 & 0 & 0 & 0 & 0 \\ -1 & -1 & 0 & 0 & -1 & -1 & 0 & 0 & 1 & -1 & 1 & 1 \\ 0 & 0 & 0 & 0 & 0 & 0 & 0 & 0 & 0 & 1 & 0 & 0 \\ 0 & 0 & 0 & 0 & 0 & 0 & 0 & 0 & 0 & 1 & 0 & 0 \\ 0 & 0 & 0 & 0 & 0 & 0 & 0 & 0 & 0 & 1 & 0 & 1 \end{pmatrix}. \text{ Then } M^{-1} \partial_2 = \begin{pmatrix} 0 & 0 & 0 & 0 \\ 0 & 0 & 0 & 0 \\ 0 & 0 & 0 & 0 \\ 0 & 0 & 0 & 0 \\ 0 & 0 & 0 & 0 \\ 0 & 1 & 0 & 1 \\ 0 & 1 & 1 & 0 \\ -1 & -1 & 0 & 0 \\ -1 & -1 & 0 & 0 \\ -1 & -1 & 0 & 0 \end{pmatrix}$$

The last zero-columns of ∂_1 generate $\ker \partial_1 = \mathbb{Z}^5$. From those generators, which in the matrix $M^{-1} \partial_2$ correspond to the five last rows, three of them —the non-zero rows corresponding to the row reduction of the (non-zero lower part of $M^{-1} \partial_2$)

$$\begin{pmatrix} 1 & 0 & 0 & -1 \\ 0 & 1 & 0 & 1 \\ 0 & 0 & 1 & -1 \\ 0 & 0 & 0 & 0 \\ 0 & 0 & 0 & 0 \end{pmatrix}$$

lie also in the image of ∂_2 . It follows $H_1(\mathcal{R}_1) = \mathbb{Z}^5 / \mathbb{Z}^3 = \mathbb{Z}^2$.

Example A.2. In order to compute the homology of the the complex, one labels the graph



$$\begin{aligned} C_0(\mathcal{G}) &= \langle a, p, b, q \rangle_{\mathbb{Z}} \\ C_1(\mathcal{G}) &= \langle e_1, e_2, e_3, e_4, f_1, f_2, f_3, f_4 \rangle_{\mathbb{Z}} \\ C_2(\mathcal{G}) &= \langle \mathcal{B}_e^{12}, \mathcal{B}_f^{12}, \mathcal{B}^{23}, \mathcal{B}^{24}, \mathcal{B}^{13}, \mathcal{B}^{14}, \mathcal{B}_e^{34}, \mathcal{B}_f^{34} \rangle_{\mathbb{Z}} \\ C_3(\mathcal{G}) &= \langle \mathcal{B}^1, \mathcal{B}^2, \mathcal{B}^3, \mathcal{B}^4 \rangle_{\mathbb{Z}} \end{aligned}$$

where \mathcal{B}^c means omission of the color c . The differentials of the chain complex

$$0 \rightarrow C_3(\mathcal{G}) \simeq \mathbb{Z}^4 \xrightarrow{\partial_3} C_2(\mathcal{G}) \simeq \mathbb{Z}^8 \xrightarrow{\partial_2} C_1(\mathcal{G}) \simeq \mathbb{Z}^8 \xrightarrow{\partial_1} C_0(\mathcal{G}) \simeq \mathbb{Z}^4 \rightarrow 0$$

are explicitly:

$$\partial_1 = \begin{pmatrix} 0 & 0 & -1 & -1 & -1 & -1 & 0 & 0 \\ 1 & 1 & 1 & 1 & 0 & 0 & 0 & 0 \\ -1 & -1 & 0 & 0 & 0 & 0 & -1 & -1 \\ 0 & 0 & 0 & 0 & 1 & 1 & 1 & 1 \end{pmatrix}, \quad \partial_2 = \begin{pmatrix} -1 & 0 & 0 & 0 & -1 & -1 & 0 & 0 \\ 1 & 0 & -1 & -1 & 0 & 0 & 0 & 0 \\ 0 & 0 & 1 & 0 & 1 & 0 & -1 & 0 \\ 0 & 0 & 0 & 1 & 0 & 1 & 1 & 0 \\ 0 & -1 & 0 & 0 & -1 & -1 & 0 & 0 \\ 0 & 1 & -1 & -1 & 0 & 0 & 0 & 0 \\ 0 & 0 & 1 & 0 & 1 & 0 & 0 & -1 \\ 0 & 0 & 0 & 1 & 0 & 1 & 0 & 1 \end{pmatrix}, \quad \partial_3 = \begin{pmatrix} 0 & 0 & 1 & 1 \\ 0 & 0 & 1 & 1 \\ 1 & 0 & 0 & 1 \\ -1 & 0 & 1 & 0 \\ 0 & 1 & 0 & -1 \\ 0 & -1 & -1 & 0 \\ 1 & 1 & 0 & 0 \\ 1 & 1 & 0 & 0 \end{pmatrix}$$

To compute H_2 , the reduced versions are

$$\partial'_2 = \begin{pmatrix} 1 & 0 & 0 & 0 & 0 & 0 & 0 & 0 \\ 0 & 1 & 0 & 0 & 0 & 0 & 0 & 0 \\ 0 & 0 & 1 & 0 & 0 & 0 & 0 & 0 \\ -1 & -1 & -1 & 0 & 0 & 0 & 0 & 0 \\ 0 & 0 & 0 & 1 & 0 & 0 & 0 & 0 \\ 1 & 1 & 0 & -1 & 0 & 0 & 0 & 0 \\ 0 & 0 & 0 & 0 & 1 & 0 & 0 & 0 \\ -1 & -1 & 0 & 0 & -1 & 0 & 0 & 0 \end{pmatrix} \quad \partial'_3 = \begin{pmatrix} 0 & 0 & 0 & 0 \\ 0 & 0 & 0 & 0 \\ 0 & 0 & 0 & 0 \\ 0 & 0 & 0 & 0 \\ 0 & -1 & -1 & 0 \\ 0 & 1 & 0 & -1 \\ 1 & 1 & 0 & 0 \end{pmatrix} \sim \begin{pmatrix} 0 & 0 & 0 & 0 \\ 0 & 0 & 0 & 0 \\ 0 & 0 & 0 & 0 \\ 0 & 0 & 0 & 0 \\ 1 & 0 & 0 & 1 \\ 0 & 1 & 0 & -1 \\ 0 & 0 & 1 & 1 \end{pmatrix}$$

The non-zero part of ∂'_3 has rank three, whence $H_2(\mathcal{G}) = \mathbb{Z}^3/\mathbb{Z}^3 = 0$. Similarly one finds $H_1(\mathcal{G}) = 0$.

APPENDIX B. THE CELL COMPLEX OF A RIBBON GRAPH

Departing from the abstract definition, we construct here the cell-decomposition of the surface where a ribbon graph can be drawn on. To begin with, we remark that vertices do not have naturally an orientation, but only a cyclic order — so far, these are only abstract combinatorial objects. However, when one tries to represent graphs by drawings, thus evoking the orientation of the plane (counterclockwise), graphs might be given a neater representation if we invert the cyclic order on some vertices and, of course, keep track of this action with help of a sign, ϵ . Write $\epsilon_v = +1$ if we preserve the order of a vertex v as the levorotation, and $\epsilon_v = -1$ if the cyclic order of v is written as a dextrorotary vertex. The ‘fat graph’ representation of \mathcal{R} is in a natural way a cell-complex, $X(\mathcal{R})$. The skeleta $X^{(n)}$ are constructed as follows:

0-cells: Let n_v be the valence of the vertex $v \in \mathcal{R}^{(0)}$, and $\epsilon_v \in \{+1, -1\}$ its orientation. We associate v the following cyclic ordered set (see Fig. 7) of 0-cells:

$$v \rightarrow \begin{cases} (P(v)_1^+, P(v)_1^-, P(v)_2^+, P(v)_2^-, \dots, P(v)_{n_v}^+, P(v)_{n_v}^-) & \text{if } \epsilon_v = +1, \\ (P(v)_1^+, P(v)_1^-, P(v)_{n_v}^+, P(v)_{n_v}^-, \dots, P(v)_2^+, P(v)_2^-) & \text{if } \epsilon_v = -1. \end{cases} \quad (\text{B.1})$$

The 0-skeleton $X^{(0)}$ is then the union of all such points $P(v)_\alpha^\epsilon$, with v running all over $\mathcal{R}^{(0)}$, $\epsilon = \pm$ and $\alpha = 1, \dots, n_v$. One has thus, in total, $2 \sum_{v \in \mathcal{R}^{(0)}} n_v$ 0-cells.

1-cells: In order to construct $X^{(1)}$, we proceed in two steps:

- i) First, add a 1-cell \overline{pq} to for each consecutive pair of points p and q , with the order given by the cycles (B.1). That is, add for each vertex v the following cells:

$$\overline{P(v)_1^+ P(v)_1^-}, \overline{P(v)_1^- P(v)_2^+}, \dots, \overline{P(v)_{n_v}^+ P(v)_{n_v}^-}, \overline{P(v)_{n_v}^- P(v)_1^+} \quad (\epsilon_v = +1) \quad (\text{B.2})$$

$$\overline{P(v)_1^+ P(v)_1^-}, \overline{P(v)_1^- P(v)_{n_v}^+}, \dots, \overline{P(v)_2^+ P(v)_2^-}, \overline{P(v)_2^- P(v)_1^+} \quad (\epsilon_v = -1) \quad (\text{B.3})$$



(A) For a positively orientable vertex $(v, +) \in \mathcal{R}^{(0)}$, with $n_v = 6$.

(B) For a, say, valence-4 vertex, the associated 0-cells.

FIGURE 7. On the construction of the 0-skeleton, $X^{(0)}$ of \mathcal{R} .

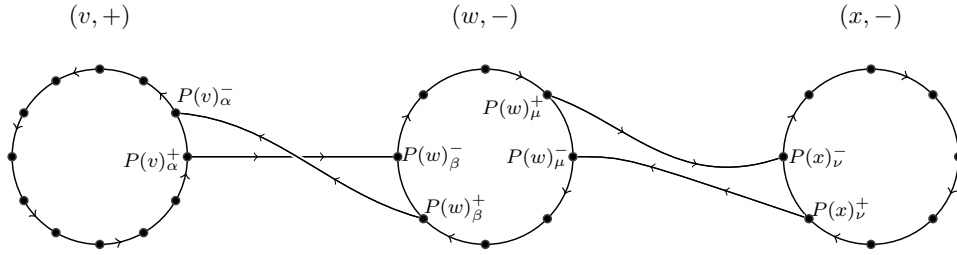


FIGURE 8. Shows the most general case on how to adjoint 1-cells. First, to the cyclic structure in eq. (B.1) (in the figure, the circles). Here the 1-cells attached to an edge e that connects with $e = [(v, \alpha), (w, \beta)]$; the opposite orientation is responsible for the apparent crossing. On the right, the two 1-cells associated to $f \in \mathcal{R}^{(1)}$, if $f = [(w, \mu), (x, \nu)]$.

This results in the space $\sqcup_{v \in \mathcal{R}^{(0)}} (\mathbb{S}_v^1)^\pm$, where the circles is given the orientation \pm of the vertices.

- ii) The second step is attaching the ribbons: for each edge $e \in \mathcal{R}^{(1)}$ with $e = [(x, \alpha), (y, \beta)]$ (viz. connecting the vertex x at the α -th place, with y at the β -th place), attach 1-cells from $P(x)_\alpha^+$ to $P(y)_\beta^-$ and from $P(y)_\beta^+$ to $P(x)_\alpha^-$ (see Fig. 1 (B) and Fig. 8). Notice that the same edges are attached if we instead take the pair $((y, \beta), (x, \alpha))$ as representative. Since for each vertex v we attached double lines, the whole number of attached 1-cells is $2 \sum_{v \in \mathcal{R}^{(0)}} n_v + 2|\mathcal{R}^{(1)}|$.

2-cells. The last skeleton $X^{(2)}$ is obtained in two steps:

- a) filling the ribbon double lines: that is, if $e \in \mathcal{R}^{(1)}$ and $e = [(v, \alpha), (w, \beta)]$, 2-disk attachment at the loop formed by $\overline{P(v)_\alpha^+ P(v)_\alpha^-}$, $\overline{P(w)_\beta^+ P(w)_\beta^-}$ and the two ribbon segments constructed for e in step ii) above.
- b) The second step is filling for all $v \in \mathcal{R}^{(0)}$ the vertex-circles \mathbb{S}_v^1 which one gets by (B.2). In total, we added $|\mathcal{R}^{(1)}| + |\mathcal{R}^{(0)}|$ 2-cells.

This exhibits the cell-structure $X^{(2)}$ of a ribbon graph. But actually is more natural not to stop at $X^{(2)}$ and to adjoint more 2-cells to some loops left, namely the boundary components. A *boundary component* of the graph \mathcal{R} here is a loop of the graph formed by the boundary of the ribbons' long segments and arcs determined by the orientation, as pictured in Figure 9 (A) (see also Fig. 1 (B)).

Formally, these boundary components are described as follows: take an arbitrary edge $e = [(v, \alpha), (w, \beta)]$ and let $s(\alpha)$ be the next place according to the cyclic ordering given to v (i.e. $s(\alpha) \equiv \alpha \pm 1 \pmod{n_v}$ if $\epsilon_v = \pm$). Thus, consider the path that begins with the segments $\overline{P(w)_\beta^+ P(v)_\alpha^-}$, $\overline{P(v)_\alpha^- P(v)_{s(\alpha)}^+}$. We can juxtapose another segment, since there is a unique $f \in$

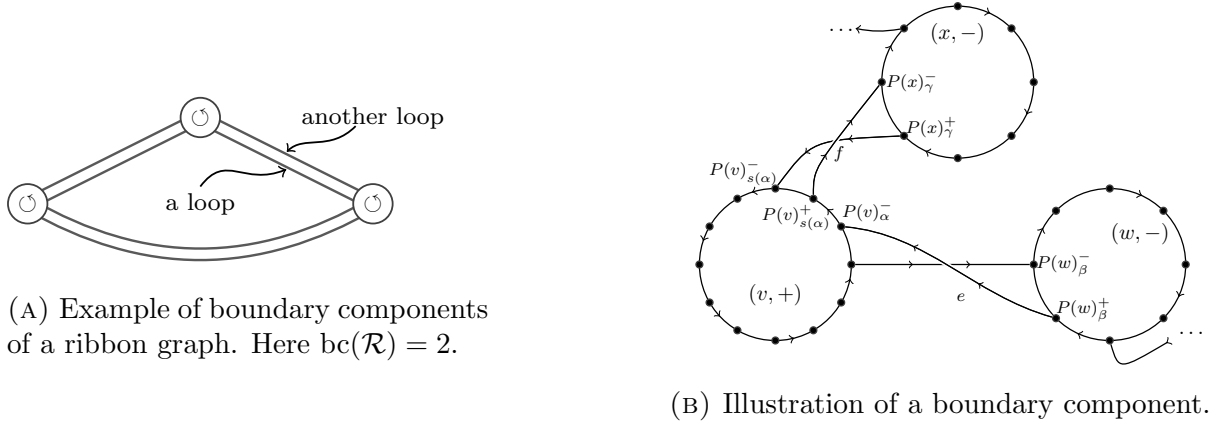


FIGURE 9. On the definition of boundary components.

$\mathcal{R}^{(1)}$ and a unique $x \in \mathcal{R}^{(0)}$ with $f = [(v, s(\alpha)), (x, \gamma)]$. The process finishes after a finite number of steps by coming back to $P(w)_\beta^+$, at the latest, when we run out of vertices. The loop ℓ_1 obtained by concatenation of these paths (see Fig. 9 (B))

$$\ell_1 = \overline{P(w)_\beta^+ P(v)_\alpha^- P(v)_{s(\alpha)}^+ P(x)_\gamma^- \dots P(w)_\beta^+}$$

is a boundary component. It might be that the not all vertices lie on ℓ_1 , so pick one such a vertex and repeat the process to get ℓ_2 . The final number of non-intersecting loops —that is, after each 0-cell $p \in X^{(0)}$ lies precisely in one of the $\ell_1, \ell_2, \dots, \ell_{\text{bc}(\mathcal{R})}$ — defines $\text{bc}(\mathcal{R})$, the *number of boundary components*.

Thus each boundary component ℓ is, by construction, homeomorphic to \mathbb{S}_ℓ^1 by certain map, say φ_ℓ . Then we attach to the ribbon picture $X^{(2)}$ a 2-cell \mathring{D}_ℓ^2 by such a map $\varphi_\ell : \partial \mathring{D}_\ell^2 \rightarrow \mathbb{S}_\ell^1$, for each $\ell = 1, \dots, \text{bc}(\mathcal{R})$. The cell-structure of $\Sigma(\mathcal{R})$ is that of \mathcal{R} but with $\text{bc}(\mathcal{R})$ more 2-cells. Thus

$$\begin{aligned} |\text{0-cells of } \Sigma(\mathcal{R})| &= 2 \sum_{v \in \mathcal{R}^{(0)}} n_v, \\ |\text{1-cells of } \Sigma(\mathcal{R})| &= 2 \sum_{v \in \mathcal{R}^{(0)}} n_v + 2|\mathcal{R}^{(1)}|, \\ |\text{2-cells of } \Sigma(\mathcal{R})| &= |\mathcal{R}^{(0)}| + |\mathcal{R}^{(1)}| + \text{bc}(\mathcal{R}). \end{aligned}$$

Since we have a finite cell-complex, we conclude from this:

$$\chi(\Sigma(\mathcal{R})) = \sum_j (-1)^j |j\text{-cells of } \Sigma(\mathcal{R})| = |\mathcal{R}^{(0)}| - |\mathcal{R}^{(1)}| + \text{bc}(\mathcal{R}).$$

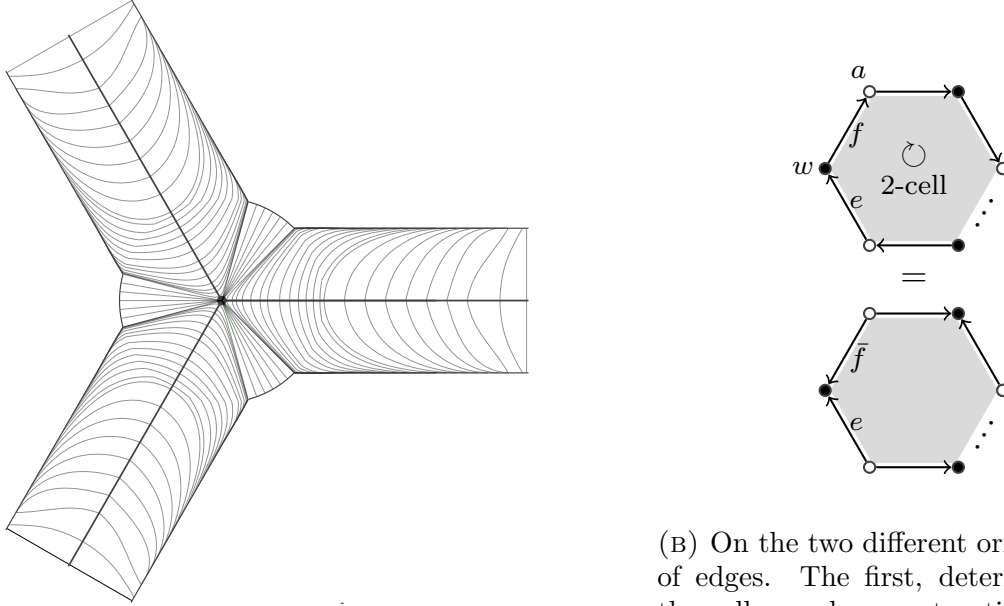
Since \mathcal{R} has been assigned a cell-structure as well, ‘ $\chi(\mathcal{R})$ ’ is now misleading. It will *not* denote $\chi(X(\mathcal{R}))$ but $\chi(\Sigma(\mathcal{R}))$, as in stated in Definition 2.16.

Remark B.1. Notice that, by construction, the inclusion of the cell-complex into a closed, compact surface $\Sigma(\mathcal{R})$ is an embedding $X(\mathcal{R}) \hookrightarrow \Sigma(\mathcal{R})$.

The next result is nothing unexpected. It shows that the two definitions of Euler characteristic harmonically coexist:

Proposition B.2. *The Euler characteristic of a 3-colored graph is the same, either if we compute it by its bubble homology or, by appealing its ribbon graph structure, via its geometric realization.*

Proof. Let \mathcal{G} be a 3-colored graph. Because of Lemma 2.18, we can consider the cell complex $X(\mathcal{G})$ embedded in the ribbon graph realization $\Sigma(\mathcal{G})$. We transform $\Sigma(\mathcal{G})$ into another cell-complex $Y(\mathcal{G})$ by a deformation retraction. We retract the ribbons’ disks to thin edges and the



(A) On local coordinates, the deformation retraction $\Sigma(\mathcal{G}) \rightarrow Y(\mathcal{G})$ on a neighborhood of a vertex. The disk is continuously collapsed to a point-like vertex, and the ribbons sent to the (1-dimensional) half-edges as shown.

(B) On the two different orientations of edges. The first, determined by the cell-complex construction of ribbon graphs (above) and the lower one by the cell-attachment by bubble homology, see eq. (2.10) with $p = 2$.

FIGURE 10. On the proof of Proposition B.2.

vertices' disks to actual point-like vertices; see Fig. 10 (A). We end up with

$$|0\text{-cells}| = |\mathcal{G}^{(0)}|, \quad |1\text{-cells}| = |\mathcal{G}^{(1)}|, \quad |2\text{-cells}| = \text{bc}(\mathcal{G}).$$

We claim that the complex associated to $Y(\mathcal{G})$ is the same cell-complex obtained by bubble homology.

For cells of dimensions $p = 0, 1$, the statement is trivially verified, since a graph is, naturally, a cell-complex. For dimension 2, we observe that each boundary component we attached 2-cells to, was formed by arcs on the disks, and segments on the next edge (determined by the cyclic ordering at the vertex). After the deformation retraction, the arcs no longer exist. Therefore the boundary component is now composed by the 1-cells determined by only the edges as follows. Pick a boundary component and an arbitrary edge e lying on it. Let c be the color of e . Then pick the black vertex (name it w) e is attached to. The next edge f has then color $c - 1 \pmod{3}$, since w has orientation (321). By the same token, f is attached to a white vertex, say a , that determines the next edge lying on the boundary component; this has color c again, for a has been assigned the orientation (123). This yields then a sequence of edges that forms connected path of edges of alternating colors $\{c, c - 1\}$. Thus, each one of the attached 2-cells to the boundary components of $X(\mathcal{G})$ corresponds, after the deformation retraction, to a bicolored connected path. These are, by definition, 2-bubbles. Therefore $C_2(Y(\mathcal{G})) = C_2(\mathcal{G})$.

On the equivalence of the boundary operators: The boundary operator $\partial'_2 : C_2(Y(\mathcal{G})) \rightarrow C_1(Y(\mathcal{G}))$ is the sum of all edges that lie on a boundary component, with 'compatible orientation' (that is, if the edges e and f meet at the vertex w , then f and e point in opposite directions, as seen from w). Since any generator of $C_2(Y(\mathcal{G}))$ is of the form $\mathcal{B}^{(ij)}$, with $i < j$,

$$\begin{aligned} \partial'_2(\mathcal{B}^{(ij)}) &= \sum_{\text{all edges, } e_c \subset \mathcal{B}^{(ij)}} e_c = \sum_{e \in \mathcal{G}_i^{(1)}} e + \sum_{f \in \mathcal{G}_j^{(1)}} f \\ &= \sum_{e \in \mathcal{G}_i^{(1)}} e - \sum_{f \in \mathcal{G}_j^{(1)}} \bar{f} = \partial_2(\mathcal{B}^{(ij)}). \end{aligned}$$

where \bar{f} is the edge with the opposite orientation (cf. Fig. 10 (B)). □

REFERENCES

- [1] Jan Ambjørn, Bergfinnur Durhuus, and Thordur Jonsson. Three-dimensional simplicial quantum gravity and generalized matrix models. *Mod. Phys. Lett.*, A6:1133–1146, 1991.
- [2] M. Atiyah. Topological quantum field theories. *Inst. Hautes Etudes Sci. Publ. Math.*, 68:175–186, 1989.
- [3] John C. Baez. Spin network states in gauge theory. *Adv. Math.*, 117:253–272, 1996. arXiv:gr-qc/9411007.
- [4] John W. Barrett and Lisa Glaser. Monte Carlo simulations of random non-commutative geometries. *J. Phys.*, A49(24):245001, 2016. arXiv:1510.01377.
- [5] Joseph Ben Geloun and Vincent Rivasseau. A Renormalizable 4-Dimensional Tensor Field Theory. *Commun. Math. Phys.*, 318:69–109, 2013. arXiv:1111.4997.
- [6] Joseph Ben Geloun and Dine Ousmane Samary. 3D Tensor Field Theory: Renormalization and One-loop β -functions. *Annales Henri Poincare*, 14:1599–1642, 2013. arXiv:1201.0176.
- [7] Valentin Bonzom, Răzvan Gurău, Aldo Riello, and Vincent Rivasseau. Critical behavior of colored tensor models in the large N limit. *Nucl. Phys.*, B853:174–195, 2011. arXiv:1105.3122.
- [8] Valentin Bonzom, Răzvan Gurău, and Vincent Rivasseau. Random tensor models in the large N limit: Uncoloring the colored tensor models. *Phys. Rev.*, D85:084037, 2012. arXiv:1202.3637.
- [9] Sylvain Carrozza. Flowing in group field theory space: a review. *SIGMA*, 2016. arXiv:1603.01902.
- [10] Sylvain Carrozza, Daniele Oriti, and Vincent Rivasseau. Renormalization of a SU(2) Tensorial Group Field Theory in Three Dimensions. *Commun. Math. Phys.*, 330:581–637, 2014. arXiv:1303.6772.
- [11] Sylvain Carrozza and Adrian Tanasă. $O(N)$ Random Tensor Models. 2015. arXiv:1512.06718.
- [12] Ali H. Chamseddine and Alain Connes. The Spectral action principle. *Commun. Math. Phys.*, 186:731–750, 1997.
- [13] Ali H. Chamseddine, Alain Connes, and Matilde Marcolli. Gravity and the standard model with neutrino mixing. *Adv. Theor. Math. Phys.*, 11(6):991–1089, 2007.
- [14] P. Di Francesco. Rectangular matrix models and combinatorics of colored graphs. *Nucl. Phys.*, B648:461–496, 2003. arXiv:cond-mat/0208037.
- [15] P. Di Francesco, Paul H. Ginsparg, and Jean Zinn-Justin. 2-D Gravity and random matrices. *Phys. Rept.*, 254:1–133, 1995. arXiv:hep-th/9306153.
- [16] M. Ferri, C. Gagliardi, and L. Grasselli. A graph-theoretical representation of pl-manifolds — a survey on crystallizations. *Aequationes Mathematicae*, 31(1):121–141, 1986.
- [17] Laurent Freidel. Group field theory: An Overview. *Int. J. Theor. Phys.*, 44:1769–1783, 2005. arXiv:hep-th/0505016.
- [18] Joseph Ben Geloun. Renormalizable Tensor Field Theories. In *18th International Congress on Mathematical Physics (ICMP2015) Santiago de Chile, Chile, July 27-August 1, 2015*, 2016. arXiv:1601.08213.
- [19] Harald Grosse and Raimar Wulkenhaar. Self-Dual Noncommutative φ^4 -Theory in Four Dimensions is a Non-Perturbatively Solvable and Non-Trivial Quantum Field Theory. *Commun. Math. Phys.*, 329:1069–1130, 2014. arXiv:1205.0465.
- [20] Răzvan Gurău. Colored Group Field Theory. *Commun. Math. Phys.*, 304:69–93, 2011. arXiv:0907.2582.
- [21] Răzvan Gurău. The $1/N$ expansion of colored tensor models. *Annales Henri Poincare*, 12:829–847, 2011. arXiv:1011.2726.
- [22] Răzvan Gurău. A review of the large- N limit of tensor models. *Symmetries and Groups in Contemporary Physics*, 2012. arXiv:1209.4295.
- [23] Răzvan Gurău. The complete $1/N$ expansion of colored tensor models in arbitrary dimension. *Annales Henri Poincare*, 13:399–423, 2012. arXiv:1102.5759.
- [24] Răzvan Gurău. Universality for Random Tensors. *Ann. Inst. H. Poincare Probab. Statist.*, 50(4):1474–1525, 2014. arXiv:1111.0519.
- [25] Răzvan Gurău and James P. Ryan. Colored Tensor Models - a review. *SIGMA*, 8:020, 2012. arXiv:1109.4812.
- [26] Matilde Marcolli and Walter D. van Suijlekom. Gauge networks in noncommutative geometry. *Journal of Geometry and Physics*, 75:71 – 91, 2014. arXiv:1301.3480 [math-ph].
- [27] Edwin E. Moise. Affine Structures in 3-Manifolds: V. The Triangulation Theorem and Hauptvermutung. *Annals of Mathematics*, 56(1):96–114, 1952.

- [28] M. Mulase and M. Penkava. Ribbon graphs, quadratic differentials on Riemann surfaces, and algebraic curves defined over $\overline{\mathbb{Q}}$. *Asian J. Math.*, 2(4):875–919, 1998.
- [29] nLab. <https://ncatlab.org/nlab/show/ribbon+graph>.
- [30] Daniele Oriti. Group Field Theory and Loop Quantum Gravity. 2014. arXiv:1408.7112.
- [31] Dine Ousmane Samary. Beta functions of $U(1)^d$ gauge invariant just renormalizable tensor models. *Phys. Rev.*, D88(10):105003, 2013. arXiv:1303.7256.
- [32] Dine Ousmane Samary, Carlos I. Pérez-Sánchez, Fabien Vignes-Tourneret, and Raimar Wulkenhaar. Correlation functions of a just renormalizable tensorial group field theory: the melonic approximation. *Class. Quant. Grav.*, 32(17):175012, 2015. arXiv:1411.7213.
- [33] Carlos I. Pérez-Sánchez. The full Ward-Takahashi Identity for colored tensor models. 2016. arXiv:1608.08134 [math-ph].
- [34] Mario Pezzana. Sulla struttura topologica delle varietà compatte. *Ati Sem. Mat. Fis. Univ. Modena*, 23(1):269–277 (1975).
- [35] Vincent Rivasseau. The Tensor Theory Space. *Fortsch. Phys.*, 62:835–840, 2014. arXiv:1407.0284.
- [36] Vincent Rivasseau. Random Tensors and Quantum Gravity. *SIGMA*, 12:069, 2016. arXiv:1603.07278.
- [37] James P. Ryan. Tensor models and embedded Riemann surfaces. *Phys. Rev.*, D85:024010, 2012. arXiv:1104.5471.
- [38] Dine Ousmane Samary. Closed equations of the two-point functions for tensorial group field theory. *Class. Quant. Grav.*, 31:185005, 2014. arXiv:1401.2096.
- [39] Dine Ousmane Samary and Fabien Vignes-Tourneret. Just Renormalizable TGFT's on $U(1)^d$ with Gauge Invariance. *Commun. Math. Phys.*, 329:545–578, 2014. arXiv:1211.2618.
- [40] Adrian Tanasă. Multi-orientable Group Field Theory. *J. Phys.*, A45:165401, 2012. arXiv:1109.0694.
- [41] Adrian Tanasă. The multi-orientable random tensor model, a review. 2015. arXiv:1512.02087.

MATHEMATISCHES INSTITUT DER WWU MÜNSTER, GERMANY
E-mail address: c_pere03@uni-muenster.de